Recent Developments in Friction Stir Welding Tools for Weld Bead Defects Minimization – A Review

Surendra Kumar Lader[1] , Mayuri Baruah[1] , Raj Ballav[1] , Swarup Bag[2]

[1] National Institute of Technology, Production and Industrial Engineering Department, Jamshedpur, India.
[2] Indian Institute of Technology, Mechanical Engineering Department, Guwahati, India.

Abstract: Friction stir welding (FSW) is considered one of the most prominent methods for joining ductile materials. In this process, joining occurs in a plastic state without melting the base metals. Therefore, there is a lack of solidification cracking and shrinking of friction stir weld joints. Although, the improper stirring action of the FSW tool reduces the frictional heat input and flow of plasticized material, which deteriorates the weld joint quality. Insufficient and excessive heat input both results in the formation of weld flaws. The FSW is assisted with various new supporting tools to reduce weld flaws. The main objective of this paper is to provide collective information regarding supportive tool systems employed with FSW for the mitigation or elimination of weld flaws. FSW tool systems such as non-rotational shoulder assisted FSW, counter-rotating twin tool, reverse dual rotation, self-reacting tool, and in-situ rolling tool, and their impact on the weld joint formation is presented in this article. This paper also presented an overview of the remarkable effect of optimizing the FSW process parameters and the influence of tool pin profiles on weld joint quality. From this review, it is concluded that various FSW supporting tool systems significantly reduce the weld flaws.

Key-words: FSW; Supporting tool systems; Material flow; Stirring effect, Defect.

1. Introduction

Friction stir welding (FSW) was developed and patented by The Welding Institute (UK) in 1991 [1]. The FSW process is named a "Green technique" because this process does not have any adverse effect on the environment [2]. The FSW tool consists of a pin and a shoulder, as depicted in Figure 1. The pin and shoulder lower surfaces generate frictional heat due to the rotating action of the tool. The heat generated in the process is 60-80% of the base metal's melting point [3,4]. Plasticized material in the front of the FSW tool is then extruded around the pin and mechanically mixed to form a joint. For the welding of aluminum alloys, several fusion welding techniques are available. But, the application of these welding techniques is found limited due to melting and solidification-related defects. A solid-state welding technique such as FSW could solve these problems. The 6000, 2000, and 5000 series of aluminum alloys are the most popular aluminum alloys due to their stress corrosion cracking resistance, high strength to weight ratio, good machining properties, and stiffness and fatigue resistance. FSW is one of the most preferred techniques for joining ductile materials that are hard to weld and for welding plates with dissimilar thickness [5]. Almost all ductile materials can be welded through this FSW process which reflects the flexibility and reliability of this technique.
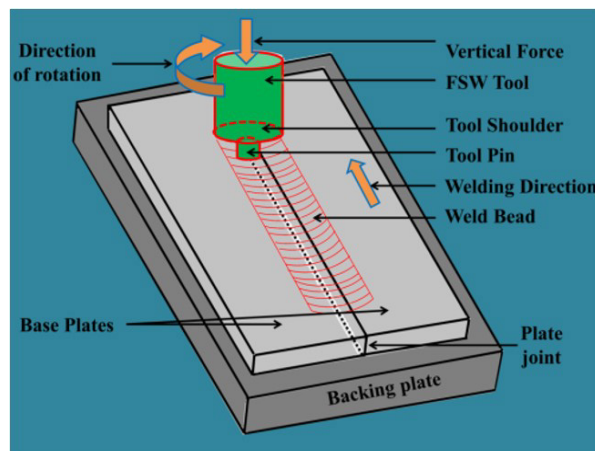

Figure 1. FSW process.

The requirement for light and high-strength materials in the automobile, aviation and shipbuilding industries is at its peak today. The FSW technique is handy for producing lightweight structures [6-8]. FSW does not require any consumable electrodes during the welding process, making the weld joint light in weight [9-12]. This technique is considered the most desirable for joining similar and dissimilar aluminum alloys [13,14]. Compared to fusion welding, the formation of weld defects in FSW is quite less, but the formation of weld flaws is still inevitable. Several authors attempted various methods to reduce the weld flaws by varying FSW process parameters, tool shoulder design, and tool pin profile. Despite several studies on the effect of FSW process parameters and tool pin profiles, there is still the formation of weld porosity, voids, cracks, tunnel defects, etc. To further minimize the imperfection of weld joint modern FSW tools were invented to enhance the weld joint quality. Material selection of the tool is an essential aspect of FSW to improve the load-bearing capacity and dimensional stability of the FSW tool [15,16]. During the welding of hard materials such as steel and titanium alloys, there is a substantial temperature rise, resulting in the wearing of the tool, which significantly affects the performance of tool and weld joint [17]. The tool pin design is another influential parameter in improving the material flow and stirring effect [18]. Several tool pin profiles are used during welding to enhance the weld joint properties [19]. FSW tools and parameters which affect the formation of weld flaws are depicted in Figure 2.

Advanced joining FSW tools, essential to any manufacturing process, are employed with FSW to access their sustainability for use in high-strength and lightweight structures [9]. In recent years several articles on FSW and its impact on the aerospace and automobile industry have been reviewed [20,21]. In the open literature, there is a lot of collective information available regarding advances in friction stir welding [22], the effect of water cooling [23], recent developments in friction stir processing [24], industrialization, and research status [25]. However, there is a lack of proper literature reviewing the roles of friction stir welding supporting tools on weld joint formation.

The present article emphasizes the FSW-assisted tool systems where material stirring occurs. The main goal of this paper is to highlight the supportive tool systems of FSW, which are beneficial for reducing weld imperfections compared to conventional FSW. Furthermore, the effect of tool pin profiles, the importance of optimizing process parameters, and their roles in enhancing the overall quality of weld joints is reported in the present article.
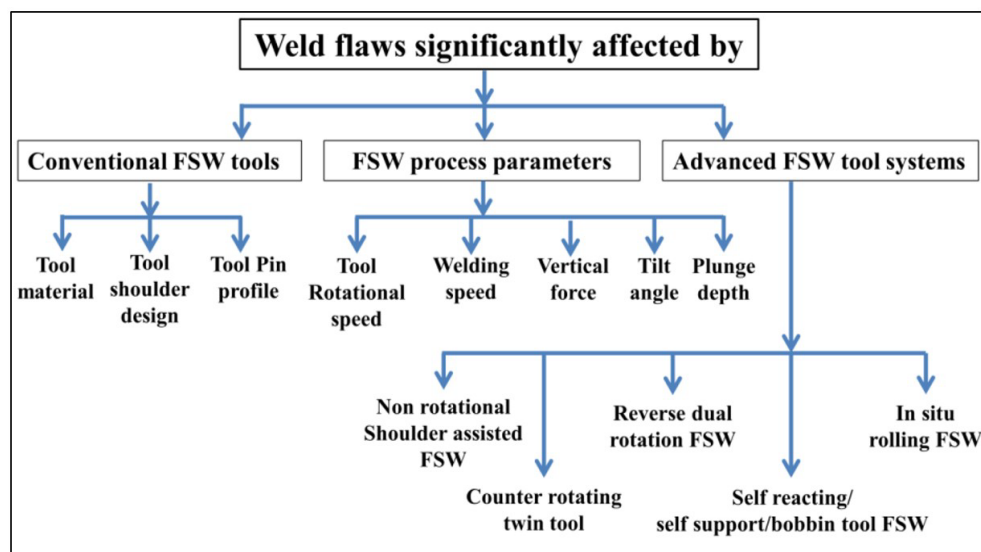

Figure 2. Classification of FSW conventional tools, advanced tools systems and FSW process parameters which affect the formation of weld flaws.

2. Significance of Conventional FSW Tool on the Formation of Weld Joint

2.1. Effect of tool material on the development of weld joint

Defects in FSW are generally formed due to improper selection of tool material, tool pin profile and FSW process parameters. Material selection of tool is an important aspect in FSW in order to improve load bearing capacity and dimensional stability of tool [26-30]. During welding of soft materials like aluminum and magnesium alloys, the most common tool material employed during FSW are mentioned in the Table 1. For high strength aluminum alloys such as AA2024 and AA7075, there is substantial rise in temperature which results in wearing of tool which significantly affect the performance of tool and weld joint as well [17,30]. During FSW of hard materials, the FSW tool deform and material from the tool detached and mixes in the weld zone in the form of fragments. These fragments are also one of the main reasons of forming weld defects in the FSW stirred zone due to difference in the melting temperature of tool material and base metal. It is difficult to apply FSW to hard materials like steel and titanium alloys because of excessive tool wear throughout the process. During the plunge phase the tool wears out the most. Additionally, the iron present in these FSW tool made up of tool steels mixes with the aluminum at the stirred

zone (SZ) and form Fe-Al composites [26-30]. Fe-Al composites are brittle in nature and deteriorate the FSW joint quality. Wear is caused by the FSW tool rotation and translation through the workpiece. The FSW tool may also distort plastically as a result of a drop in its yield strength at high temperatures and heavy loads. Tool failure may occur when the stresses exceed the tool's capacity to support the load. A threaded AISI oil-hardened steel tool wearing is shown in Figure 3 formed during the FSW of Al6061 [31]. However, it has been noted that after the initial wear, the wear rates of FSW tool significantly reduce and produces smoothed surface (or self-optimized) tool as depicted in Figure 3, which may also continue to produce high-quality welds [31,32].

Table 1. Common tool materials used for FSW of soft metals.

| Tool Material	Work piece material
Mild Steel	Magnesium alloys
High Carbon Steel	Magnesium alloys
Armour Steel	Magnesium alloys
Stainless Steel	Magnesium alloys
AISI 4140	Dissimilar materials
AISI oil hardened tool steel	Aluminum matrix composite materials
High Speed Steel	Magnesium alloys
Tool Steel	Aluminum alloys, Dissimilar materials
H13 Steel	Magnesium alloys
SKD61 Tool Steel	Dissimilar materials
High Carbon High Chromium Steel	Magnesium alloys, Aluminum alloys, Dissimilar materials
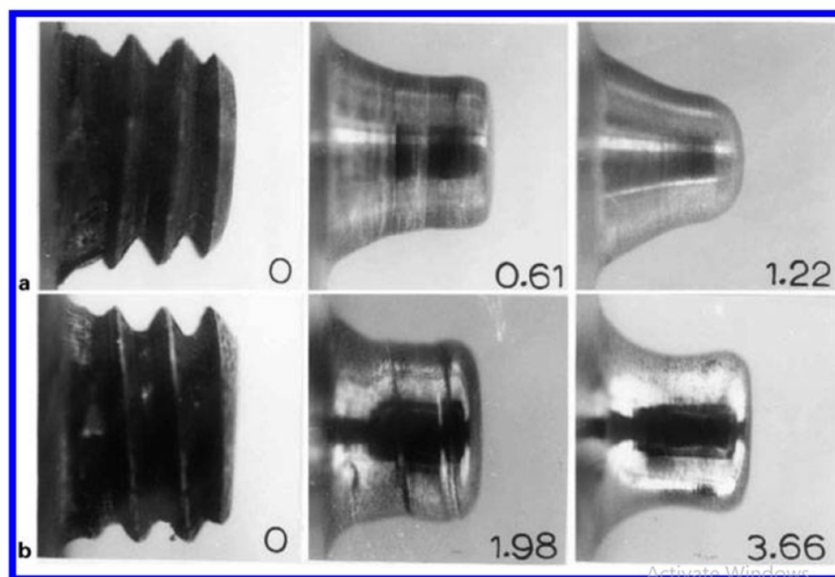
Figure 3. Evolution of tool wear in the FSW of AA6061 with 01 AISI oil hardened tool steel at 1000 rpm rotational speed and welding speed of (a) 3 mm/sec (b) 9mm/sec: distances travelled by tool in meters are indicated in right below for each tool [31].

The hardening of FSW tool was recommended prior to FSW to eliminate the deformation during FSW. Most of the FSW tools were made up of tool steels such as stainless steel, D2, D3 and H13 [26-30]. Despite, the fact that it is frequently employed to weld aluminum and other soft metals, the applicability of FSW to hard alloys like steels and titanium alloys is limited due to premature tool failure. It was discovered that the kind of tool coating significantly influence the mechanical, metallurgical, and stress distribution characteristics of the welding zone [32]. Cevik et al. reported that the samples created by the uncoated tool and the TiN-coated tool at different rotational speeds, smooth and fine grains developed in the weld joint [32], depicted in the Figure 4. As compared to an untreated tool, the TiN-coated tool generates less heat input into the joint and makes the tool wear resistant which significantly reduces the inclusion defects [32]. It was discovered that the kind of tool coating had an impact on the mechanical, metallurgical, and stress distribution characteristics of the welding zone. On the retreating side of the samples created by the uncoated stirring tool and the TiN-coated stirring tool at different rotational speeds, micro-void flaws and broad grain bands developed. As compared to an untreated tool, the TiN-coated tool provided less heat input into the joint.

At high temperatures, severe plastic deformation occurs which resulted into the formation of flash defects [26-30]. The best tool pin geometry for a certain set of welding variables, tool and work-piece materials, can be identified based on its load bearing capability and its wear resistance. Furthermore, to improve the material flow and stirring effect the tool pin design is another influential parameter [18]. Several types of shoulder design and tool pin profiles are used during welding in order to enhance the weld joint properties [19,33,34] which are discussed in further sections.
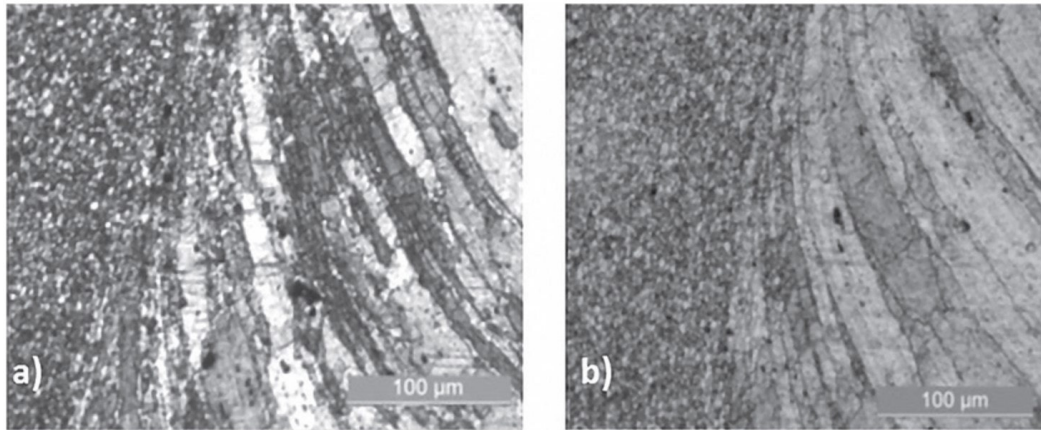

Figure 4. Effect of tool coating on microstructure of AA7075-T651 for (a) uncoated tool (b) TiN coated tool at 900rpm tool rotational speed [32].

2.2. Effect of tool shoulder geometry and pin geometry on the weld joint quality

Material mixing, heat generation, plunge force, and overall consistency of the joint are greatly influenced by the tool design [35,36]. The tool shoulder produces frictional heat and prevents material from escaping the weld zone [19,37]. Optimum shoulder design is necessary to attain adequate frictional heat input during FSW [38]. Several FSW tool shoulder design depicted in the Figure 5 were opted nowadays to enhance the surface mixing and adequate heat generation. As compared to the flat shoulder, the concave shoulder shown in the Figure 5 produces quality welds which was reported in several researches [37,39,40]. During plunging of FSW tool, the material displaced by the pin is fed into the cavity within the tool shoulder. Further the forward motion of the tool forces new material into the cavity of the shoulder, pushing the existing material into the flow of pin. This type of shoulder design significantly eliminates the voids and tunnel defect [41]. In addition to the shoulder design the diameter of shoulder also plays a crucial role for the heat generation [42]. Higher shoulder diameter increases the pressure force and heat input. Excessive heat input results in the formation of flashes and void defects. Reduction in shoulder diameter improves the joint quality microstructural properties [43]. From the several researches, the ideal shoulder design for FSW was found to be about 3 to 1.33 times the tool pin diameter [42].
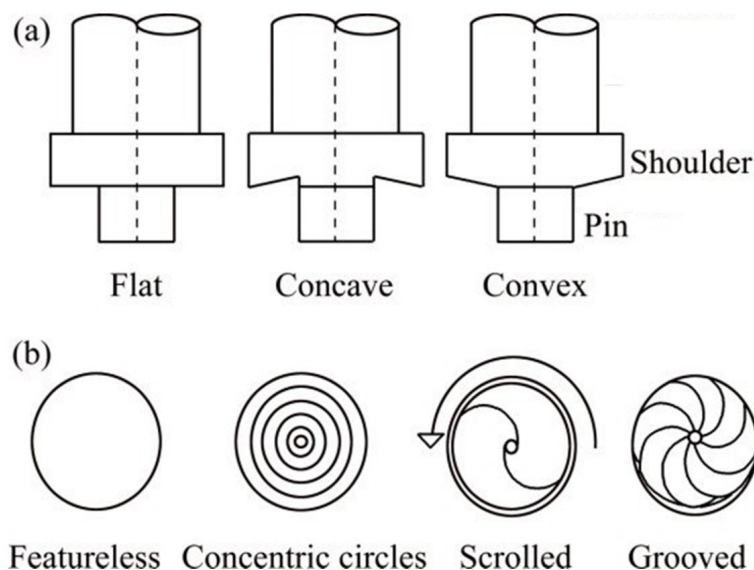

Figure 5. Different types of FSW tool shoulder (a) and shoulder bottom surface features (b) [39].

Tool pin profile plays a vital role in achieving sound weld joint during the FSW process. Tool pin performs the mechanical movement of material, mixing, and stirring action. The various tool pin profiles are used during the welding process to enhance the stirring effect and overall quality of the weld joint. The influence of tool pin profile on the development of weld joint are mentioned in the Table 2. Some tool pin profiles are cylindrical, tapered, threaded, grooved, fluted [48,49], etc. A homogeneous flow of material with good mechanical properties is obtained in a threaded pin [48]. Grooves in the pin reduce grain size and increase weld strength [50]. In square frustum pin profiles, improved hardness and uniform mixing at the weld region are attained [49]. Reduction in shoulder diameter improves microstructural properties [43]. At high tool rotational speeds, the straight square pin profile enhances mechanical properties [44]. The proper selection of tool pin profile and shoulder diameter increases the bonding surface area and strength of weld [54]. Inclination of tool and pin diameter have significant effect on the welding forces especially in vertical and transverse direction [55].

Thomas et al. [51] demonstrated the tools with inclined and fluted ridge grooves type of pin offers good weld symmetry, but the parameters need to be further optimized to obtain defect-free weld joint. The tool geometry is illustrated in Figure 6, where 'θ' is the tilt angle of the tool with respect to horizontal axis X, 'H' is the height of the shoulder, 'h' is the height of the pin, 'D' is the diameter of shoulder and 'd' is the diameter of the pin. The above mentioned tool pin profiles, such as threaded, square frustum, and fluted with ridge grooves, play a significant role in enhancing overall weld bead quality [52,56,57]. Schematic designs of some important FSW tool pin, typically used in FSW are depicted in the Figure 7. In addition to the tool material and design, the weld joint quality is also a function of FSW process parameters which is discussed below in the further sections

Table 2. Influence of tool pin profile on the weld joint quality.

| Tool pin profile	Effect on weld joint quality
Straight Cylindrical Pin	Cracks and tunnel defects are formed due to lack of vertical displacement of material [44-47].
Tapered Cylindrical Pin	Insufficient flow of plasticized material due to low heat generation per unit weld length resulted in the formation of small pinholes and tunnel defect [45-47].
Threaded Cylindrical Pin	Threaded pin profile generates sufficient heat input and enhances the downward movement of plasticized material produces defect free weld [45-48].
Square Pin	Wider SZ formed due to large amount of material sweep from the SZ which resulted in turbulent flow of material and forms tunnel defect [45-47].
Triangular Pin	Abnormal stirring occurs due to insufficient heat input at the weld root resulted in the formation of cavity at the bottom of the weld joint [45-47].
Square Frustum Pin	Uniform mixing at the weld region [49]
Fluted Ridge Groove Pin	Offers good weld symmetry and reduces the grain size which improves the strength of the weld joint [50-52]
Fluted Pin	Improper stirring and tool jamming occurs resulted in the formation of tunnel defect [53].
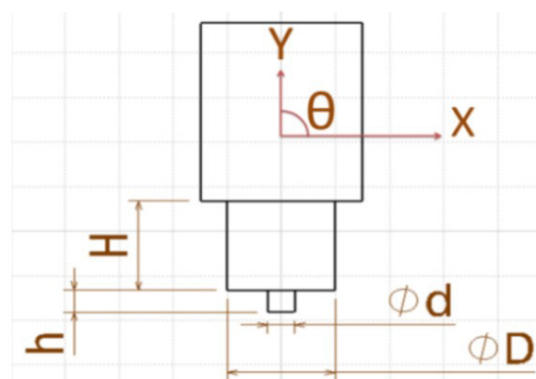
Figure 6. Tool geometry.
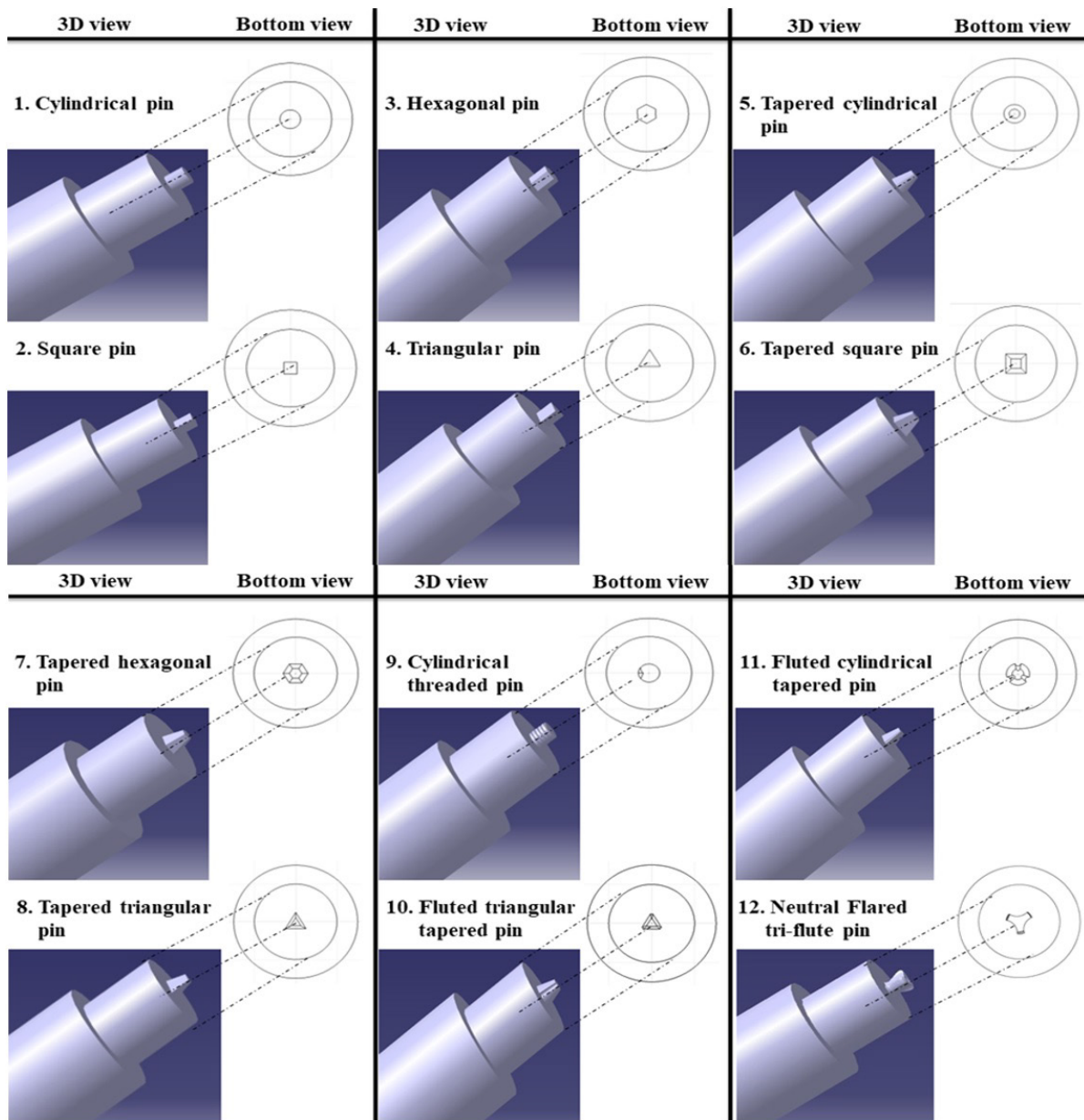
Figure 7. Types of tool pin profiles used in FSW.

3. Significance of FSW Process Parameters on the Development of Weld Joint

The FSW process parameters play a vital role in heat generation and the homogeneous mixing of materials [58]. Parameters such as tool rotational speed, transverse speed, normal force, and tool torque are properly set to attain defect-free joints [59]. The mechanical and microstructural properties, such as tensile strength, hardness, and the formation of weld flaws, are primarily attributed to these parameters [60,61]. Rotational speed is the rate of rotation of the FSW tool. According to Shojaeefard et al. [62], the overall contribution of FSW tool rotational speed in the dissimilar Al-Cu FSW system is 40%. The generation of defects, the flow of material, and tool wear are all affected by the tool rotational speed, making it a crucial process parameter in FSW. In the dissimilar FSW, Rotational speed also affects the amount of frictional heat generated, the plastic deformation of the material, and the forces on the tool. Intermetallic compounds (IMCs) formation in different Al-Cu FSW is likewise impacted by a change in a frictional heat generation. Heat input increases with increasing tool rotational speed, on the other hand, in dissimilar joining the separation of big particles in the SZ from the harder base material is caused by a stronger stirring action at a high rotational speed. These particles form a weak link with the Al matrix, which leads to flaws such cracks and voids [63-65]. Additionally, as rotational speed increases, the interfacial IMCs layer thickens due to increased heat input at the joint interface [63]. The severe rubbing action caused by the high rotational speed also shortens the tool life (for tool steel alloys) in the case of high strength alloys like brass and AA7XXX.

On the other side, very low rotating speeds induce faulty joints due to less heat input [66]. Defects, particularly macrocracks and channel defects formed in dissimilar FSW, due to inappropriate material flow because the stir zone could not plasticize

properly [63,67,68]. Moswan et al. [69] in their experimental investigation varied the rotational speed of the tool and concluded that the rotational speed of the tool significantly affects the force generation. Furthermore, they also reported that with an increase in tool rotational speed, the longitudinal force increases and the downward force decreases without any significant effect on the transverse force. Singh et al. [70] reported that the FSW process parameters strongly influence the joints' flexural strength and tensile strength. The tool rotational speed contribution is 27.88% and 58.46% in tensile and flexural strength. Palanivel et al. [44] studied the effect of FSW tool rotational speed and found that defect-free joints at higher tool rotational speed were observed at weld zone.

The pace at which a tool moves through a workpiece's joint line is known as the welding speed or travel speed. In dissimilar joining, to obtain high quality FSW joints, welding speed is also found very crucial [71,72]. It has a significant impact on the metallurgical bonding and mixing of materials in the SZ. Insufficient heat input, resulted from extremely fast welding speeds generates imperfect FSW joints [71]. Lower welding speed results in a greater heat input and formation of thick IMCs [71-73]. Turbulent flow of material in the SZ occurs at higher heat input which was the main cause of IMCs formation. These thick IMCs layer was the main cause of crack formation in the interface of dissimilar FSW joints. Improper mixing of dissimilar material in the SZ occurs at higher welding speed because it produces less heat input which resulted in the formation of void defect [71,72]. Differences in the flow stress of dissimilar materials are another cause of these problems. In order to handle the flow stress of different materials, the ideal welding speed is needed. Similar trends were observed when the welding speed was reduced while the rotational speed was kept constant [74]. It is well known that the ideal ratio of welding speed to rotational speed regulates the heat input, which in turn regulates the development of IMCs in dissimilar FSW [64,75]. According to Galvao et al. [64], the development of IMCs and the weld flaws of dissimilar FSW joints are both impacted by the ratio of rotational speed to welding speed. Rajakumar et al. [74] found that the improper selection of welding parameters leads to the formation of defects. Therefore, to enhance the weld joint quality, the FSW process parameters need to be appropriately optimized [76]. Optimization of the process parameters reduces defects' formation and enhances the weld joint's overall performance [77,78] depicted in Figure 8. The figure demonstrated that at very high tool rotational speed > 1600 rpm several weld defects such as zig-zag line and flash defects were formed in the weld zone [74,76]. Tool rotational speed of 1400 rpm produces defect-free joints. Therefore, at constant 1400 rpm when the welding speed was varied, the 60 and 80 mm/min welding speed produces defect-free weld joints. In addition to this, at higher welding speeds > 100 mm/min forms tunnel defect due to insufficient heat input. Thus, optimization of FSW process parameters plays a crucial role to enhance the weld joint quality. Lombard et al. [79] in their experimental investigation demonstrated the importance of optimizing process parameters and found that the tool rotational speed is a key parameter to enhance strength and fatigue performance of the joint. The other benefits of optimizing process parameters include improved material penetration into each other [80], low defect population [81], reduced wear of the tool and minimum residual stress generation [82].
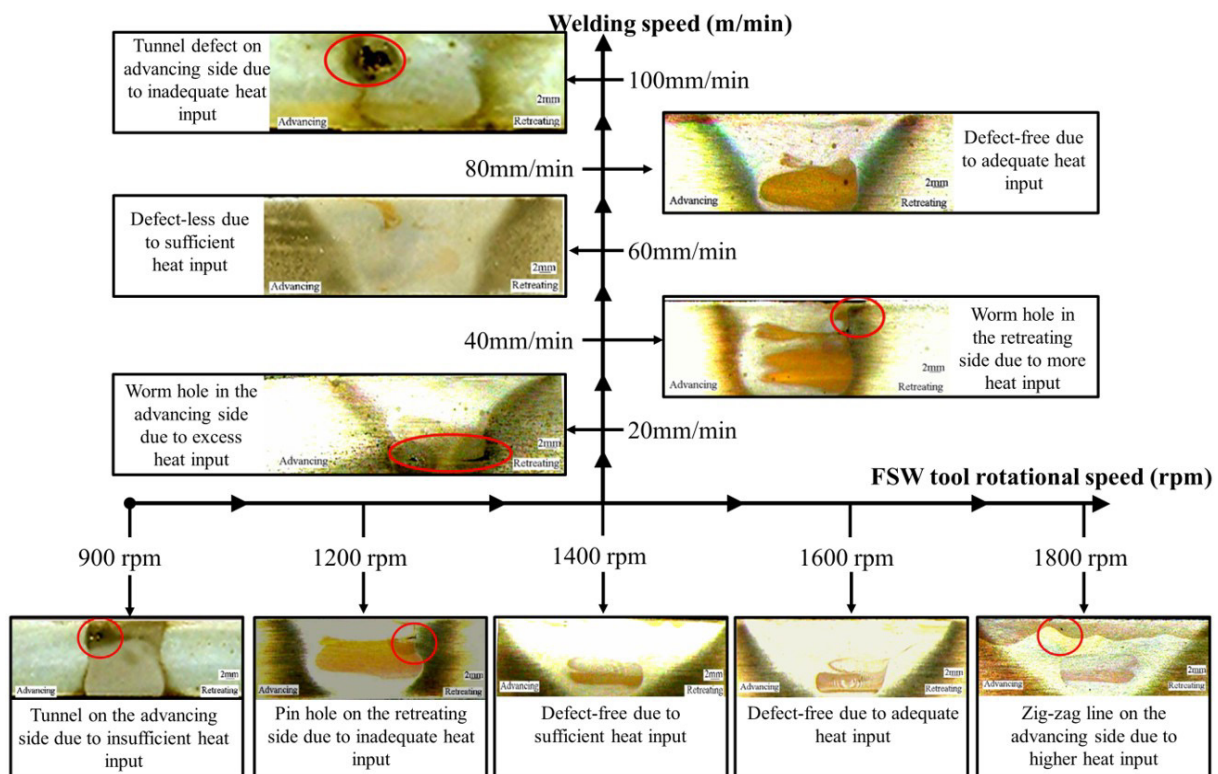

Figure 8. Effect of tool rotational speed and welding speed in the development of weld joint for AA7075-T6 [74].

In order to minimize such welding defects or to attain defect-free joints, the optimized design of overall process parameters are demonstrated in the cause and effect diagram Figure 9. Tool plunge depth and tool tilting also affects the material flow and defect formation in the SZ. Surendra et al. found that by increasing plunge depth, the heat input also increases and large flash defects were formed [83]. 0.2 mm plunge depth and 2° tilt angle were the optimized parameter reported in several literatures [83-86]. Parameter optimization is essentially useful for the materials having less weld ability such as 2000, 7000 and 5000 series of aluminum alloys [79,87]. Table 3 summarizes the types of defects obtained at various tool pin profiles and process parameters.

Despite several measures taken to use optimized FSW parameters, several defects were still reported in the weld region, which causes degradation of the weld joint [88,89]. Defect such as cavities, tunnels, and voids are formed by insufficient heat input and abnormal stirring of the tool pin [90,91]. Excess heat input leads to the formation of wider weld zone and flash defect.

In order to ensure proper heat input and enhance the weld joint quality, the FSW is assisted with various other welding techniques [92]. In dissimilar joining due to differences in melting temperatures, preheating of higher melting point material could improve the stirring effect of tool and also enhance the weld joint quality which was reported in a several studies [93-95]. Preheating is carried out by combining other welding technologies with FSW, such as plasma-assisted FSW [96], induction-assisted FSW [93], laser-assisted FSW [97], arc-assisted FSW [98], which produces a partial annealing effect and improves the plastic flow of materials. However, for adequate preheating of base metal, proper estimation of the preheating time and temperature histories is needed [99,100] because the overheating of base metals (BMs) may cause surface deformation [101] and degradation of weld joint quality [102,103]. Additionally, FSW-assisted preheating techniques consume extra energy and are not considered energy efficient, so the application of preheating in the FSW process is limited. To make the FSW process energy efficient, and to enhance the surface texture and heating conditions, various supporting tool systems [104-106] are employed in the FSW process to mitigate the weld zone imperfections. Hence, new advanced tools discussed in further sections are assisted with FSW to reduce the weld joint's defects, improving the weld joint's overall quality.
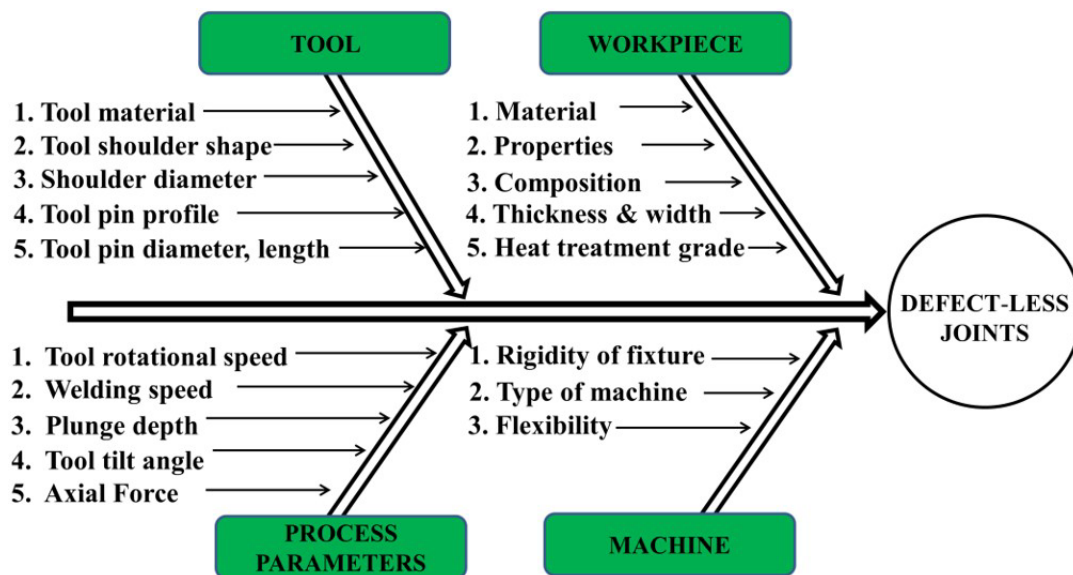
Figure 9. Cause and Effect Diagram (Fish Bone Diagram) for defect-less friction stir weld joints.

Table 3. Defects obtained at various tool pin profiles and process parameters.

Authors, Tool Pin Geometry	Process Parameters	Cross-sectional macrographs of weld zone	Type of defect and its cause
Pin geometry: Straight cylindrical -I			
Padmanaban and Balasubramanian [47] PD: 6 PL: 5.7	N: 1600 V: 40 Z: 0.2 T: 00 F: 3		Fig. I - A [47] Crack defect formed due to Lack of vertical displacement of material.
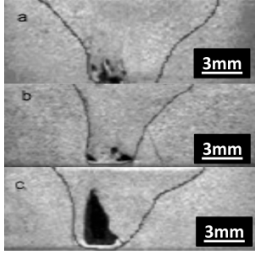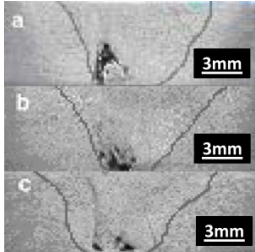
Table 3. Continued…

Authors, Tool Pin Geometry	Process Parameters	Cross-sectional macrographs of weld zone	Type of defect and its cause
Elangovan and Balasubramanian [46] PD: 6 PL: 5.7	N: 1600 V: a) 22 b) 45 c) 75 Z: NA T: NA F: 12		Fig. **I** - B [46] (a, b) Tunnel defects and pin holes are formed in the weld root towards the retreating side of the weld joint due to improper stirring of the tool pin. (c) Large tunnel defect was formed due to insufficient heat input.
Elangovan and Balasubramanian [45] PD: 6 PL: 5.7	N: a) 1500 b) 1600 c) 1700 V: 45 Z: 0.2 T: 00 F: 12		Fig. **I** - C [45] (a, b) Tunnel defects are formed at the root of the weld joint due to insufficient heat input. (c) Pin holes due to improper flow of the plasticized material.

<u>Pin geometry: Tapered cylindrical -</u> II

Authors, Tool Pin Geometry	Process Parameters	Cross-sectional macrographs of weld zone	Type of defect and its cause
Padmanaban and Balasubramanian [47] PD: 6 (root) PL: 5.7	N: 1600 V: 40 Z: 0.2 T: 00 F: 3		Fig. **II** - A [47] A long crack formed due to the absence of vertical motion of the material.
Elangovan and Balasubramanian [46] PD: 6 PL: 5.7	N: 1600 V: a) 22 b) 45 c) 75 Z: NA T: NA F: 12		Fig. **II** - B [46] (a, b) Small pinholes are formed at the bottom of the weld joint because of insufficient flow of plasticized material. (c) Tunnel defect was formed due to low heat generation per unit weld length.
Elangovan and Balasubramanian [45] PD: 6 PL: 5.7	N: a) 1500 b) 1600 c) 1700 V: 45 Z: 0.2 T: 00 F: 12		Fig. **II** - C [45] (a, c) Tunnel defect due to insufficient heat input. (b) Pin holes are formed since there is absence of vertical flow of material.

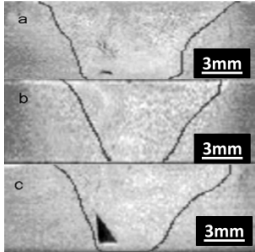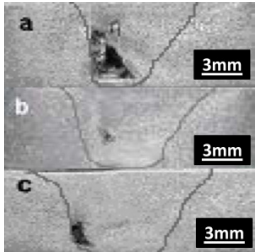**<u>Pin geometry: Threaded cylindrical -</u> III**

Authors, Tool Pin Geometry	Process Parameters	Cross-sectional macrographs of weld zone	Type of defect and its cause
Padmanaban and Balasubramanian [47] PD: 6 PL: 5.7	N: 1600 V: 40 Z: 0.2 T: 00		Fig. **III** - A [47] Defect-free joints are formed due to sufficient heat generation and proper mixing of materials.
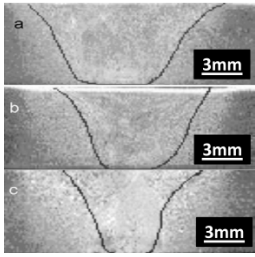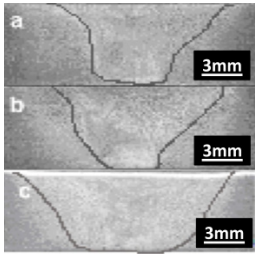
Table 3. Continued…

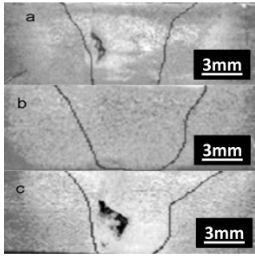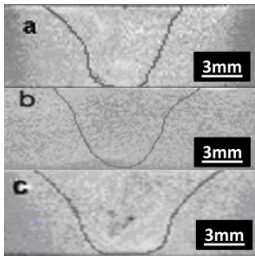| Authors, Tool Pin Geometry	Process Parameters	Cross-sectional macrographs of weld zone	Type of defect and its cause
Elangovan and Balasubramanian [46] PD: 6 PL: 5.7	F: 3 N: 1600 V: a) 22 b) 45 c) 75 Z: NA T: NA		Fig. **III** - B [46] (a) Crack-like defect formed due to excess heat input results in turbulent material flow. (b) Defect-free joint due to sufficient heat input. (c) Tunnel defect formed at the middle of the stirred zone due to faster welding speed results in lower heat input.
Elangovan and Balasubramanian [45] PD: 6 PL: 5.7	F: 12 N: a) 1500 b) 1600 c) 1700 V: 45 Z: 0.2 T: 00 F: 12		Fig. **III** - C [45] (a, b) No defect because the threaded pin profile generates sufficient heat input and enhances the downward movement of plasticized material. (c) Pin holes are formed because of excess turbulent flow of materials takes place at higher tool rotational speed.

Pin geometry: Square - IV

Authors, Tool Pin Geometry	Process Parameters	Cross-sectional macrographs of weld zone	Type of defect and its cause
Padmanaban and Balasubramanian [47] PD: NA PL: 5.7	N: 1600 V: 40 Z: 0.2 T: 00 F: 3		Fig. **IV** - A [47] Tunnel defect formed due to large amount of material sweep from the SZ.
Elangovan and Balasubramanian [46] PD: NA PL: 5.7	N: 1600 V: a) 22 b) 45 c) 75 Z: NA T: NA F: 12		Fig. **IV** - B [46] (a) Defect-free weld joint. A wider weld zone appeared due to excess heat input at a higher rotational speed. (b) Defect-free joint and adequate heat input. (c) Defect-free joint. A narrower weld zone appeared due to low heat input at lower tool rotational speed.
Elangovan and Balasubramanian [45] PD: NA PL: 5.7	N: a) 1500 b) 1600 c) 1700 V: 45 Z: 0.2 T: 00 F: 12		Fig. **IV** - C [45] (a) and (b) Defect-free joint. Adequate heat input and sufficient working of plasticized metal. (c) Defect-free joint. A wider weld zone appeared due to excess working of plasticized metal at higher tool rotational speed.

Pin geometry: Traingular - V

Authors, Tool Pin Geometry	Process Parameters	Cross-sectional macrographs of weld zone	Type of defect and its cause
Padmanaban and Balasubramanian [47] PD: NA PL: 5.7	N: 1600 V: 40 Z: 0.2		Fig. **V** - A [47] A cavity at the weld root appeared due to insufficient heat input.

Table 3. Continued…

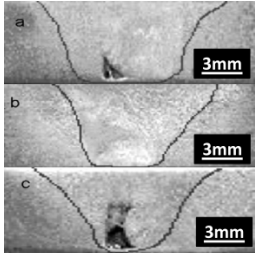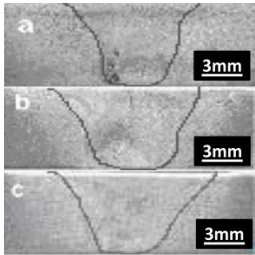| Authors, Tool Pin Geometry	Process Parameters	Cross-sectional macrographs of weld zone	Type of defect and its cause
Elangovan and Balasubramanian [46] PD: NA PL: 5.7	T: 00 F: 3 N: 1600 V: a) 22 b) 45 c) 75 Z: NA T: NA F: 12		Fig. **V** - B [46] (a) Formation of tunnel defect due to excess turbulence of the plasticized metal at higher tool rotational speed. (b) Defect-free joint. Adequate heat input and sufficient working of plasticized metal. (c) Abnormal stirring of the tool pin causes a bigger tunnel defect at the weld root towards the retreating side.
Elangovan and Balasubramanian [45] PD: NA PL: 5.7	N: a) 1500 b) 1600 c) 1700 V: 45 Z: 0.2 T: 00 F: 12		Fig. **V** - C [45] (a) Pin holes are formed towards the retreating side due to insufficient heat input. (b) Defect-free joint. Adequate heat input and sufficient working of plasticized metal. (c) Defect-free joint. Adequate heat input and sufficient working of plasticized metal.

PD = Pin diameter in mm, PL = Pin length in mm, N = Tool rotational speed in rpm, V = Welding speed, Z = Plunge depth in mm, T = Tilt angle in degree, F = Force in KN.

4. FSW Assisted Advanced tool Systems

This section highlights various supporting tool systems assisted with conventional FSW to improve joint properties. Some relevant supporting tool systems and their effect on weld quality are discussed in detail, such as non-rotational shoulder assisted FSW, counter rotating twin tool, reverse dual rotation tool, self-reacting and in-situ rolling FSW.

4.1. Non-rotational shoulder assisted friction stir welding (NRSA-FSW)

In late 2004 and early 2005, TWI proposed NRSA-FSW, another new variant of FSW, for welding high temperature and low thermal conductivity alloys, such as Ti-alloys [107,108]. In NRSA-FSW, a rotating tool is made up of a probe (with a tiny or no shoulder) that slides across the joint line during the welding process. This process is employed in order to avoid or reduce the heat produced by the shoulder depicted in Figure 10 [109]. Consequently, heat generation through the weld thickness is reduced and more concentrated in the SZ. The inherent properties of NRSA-FSW provide the following benefits.

1. The flash defects produced in traditional FSW were wiped out by and eliminated by the NRSA-FSW;

2. As compared to traditional FSW, smaller thermomechanically affected and heat affected zones (TMAZ and HAZ) were formed;

3. Root imperfections brought on by insufficient heat input were eliminated;

4. The flash defects produced in traditional FSW were wiped out by and eliminated by the NRSA-FSW;

5. Equiaxed microstructure is produced as a result of violent material flow in the weld zone;

6. The use of NRSA-FSW acts as a seal barrier which prevents plasticized material from escaping the weld site, improving material flow without affecting the effective joint thickness;

7. A symmetrical microstructure is produced at the weld center line due to lower welding temperature which was consistent throughout the thickness of weld joint.

Over the time, due to several benefits of NRSA-FSW, it has become more prominent among researchers [110-112]. Additionally, NRSA-FSW, which was earlier used to weld high strength Ti-alloys, is now used for a variety of other alloys [113-115]. Due to its unique qualities, the several researchers believe that SSFSW is now considered as the most significant joining techniques for high strength lightweight alloys.
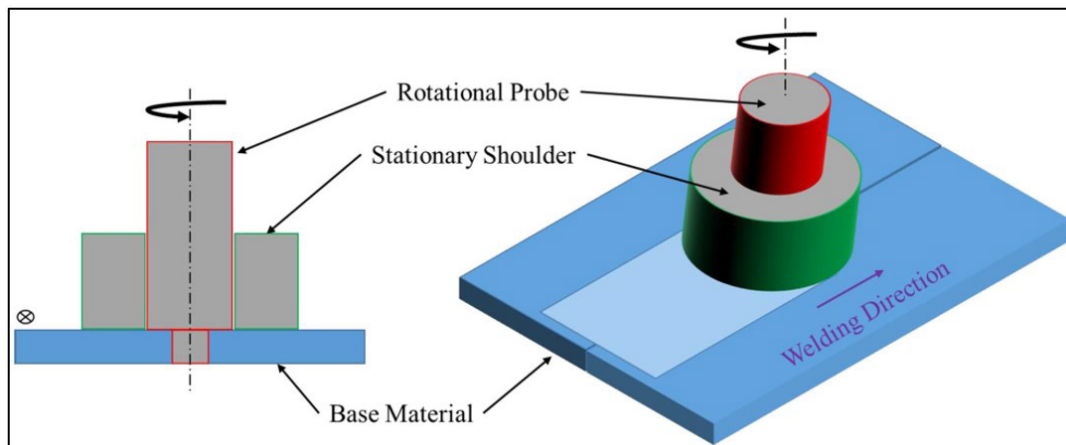
Figure 10. SSFSW process schematic in 2D section view and 3D.

Ji et al. [116], proposed a model of material flow in traditional FSW and NRSA-FSW for a lap joining of AA2024-T6 at 1000 rpm and 50 mm/min are shown in Figure 11. From the figure it was found that the cold lap and hook defect generated in traditional FSW was eliminated in NRSA-FSW. Since, in NRSA-FSW's the symmetrical and violent material flow occurs in the SZ leads to the elimination of hook and cold lap, which is the most common defects formed in FSW of lap joint [116]. Chen et al. [114], Huang et al. [117] and Xu et al. [118] showed similar types of material flow in the lap joining of AA2024, AA7075 utilising NRSA-FSW.
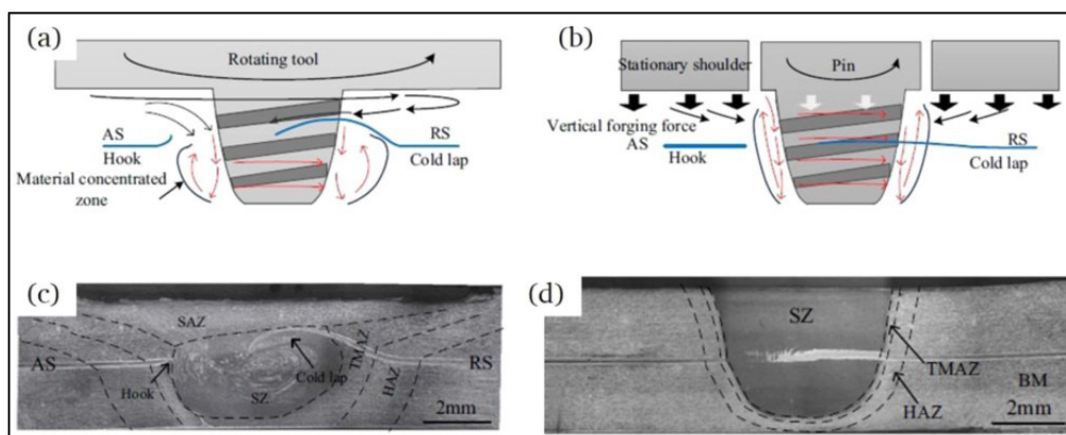
Figure 11. Material flow pattern in the lap welding of AA2024-T6 alloy using traditional FSW (a) and (c), and NRSA-FSW (b) and (d) [116].

The performance of dissimilar joints is considerably enhanced by symmetrical SZ and weaker material on the AS. Figure 12 [119] shows that the SZ of NRSA-FSW joints is reasonably symmetrical with minimum changes in BM property due to probe-dominant heat generation and material mixing. NRSA-FSW for AA2024 (2mm thick) and AA7050 (2mm thick) dissimilar joints produced joint efficiency of about 94% of AA2024-T3 at 1200 rpm and 180 mm/min. Wu et al. [120] showed that the weld thinning and pin adhesion were found negligible in similar AZ31B joints obtained in NRSA-FSW. NRSA-FSW joints showed maximum strength of 137 MPa, or 54% of AZ31B, which is 130% greater than the joint strength of FSW [120]. The remarkable effects of NRSA-FSW are mentioned in the Table 4. Moreover, the potential benefits of NRSA-FSW include improvement in joint efficiency due to violent material flow in the SZ as well as eliminate flash, hook and cold lap defects etc. Further, many more alternative tool types could be invented to investigate their motions and effects on weld joint fatigue properties.
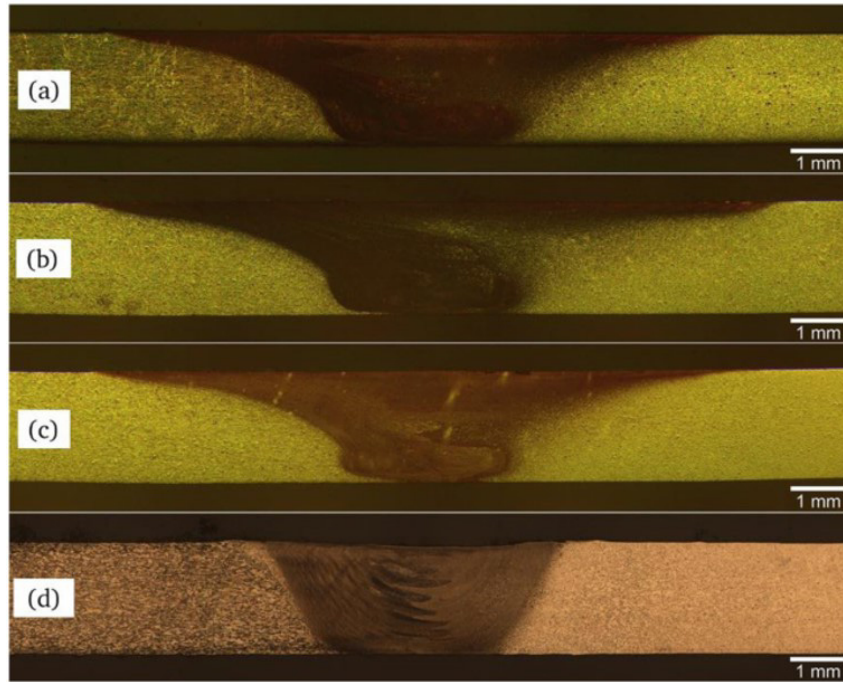
Figure 12. AA2024–AA7050 weld cross-section: FSW at 600 rpm and different welding speeds (a) 180mm/min, (b) 300mm/min, (c) 480mm/min, and (d) NRSA-FSW at 1200 rpm and 180mm/min [119].

Table 4. Remarkable effects of NRSA-FSW.

Authors	NRSA-FSW tool geometry	FSW process parameters	Remarkable effects of NRSA-FSW
Alloy, Tool Material	**a) NRS-OD/ID**		
	b) RTS-SD/PTD/PBD/PL		
	c) PP		
Li et al. [121]			1. Improve tensile strength, due to the violent material flow in the SZ and broadens process parameter range.
AA2219-T6	a) 14/10	N$_P$: 600-800	
H: 5	b) 9.8/NA/NA/4.8	V: 100	
TM: NA	c) PP: Conical threaded pin	Z: 0.2	
		T: NA	
		F: NA	
Avettand-Fènoël and Taillard [112]			1. Grain refinement occurs in post-aged heat treated samples as compared to pre-aged base metals.
AA2050-T3	a) 21.5/NA	N$_P$: 400	2. Joint efficiency shows no effect of aging sequence
H: 15	b) NA/10/NA/10	V: 100	
TM: NA	c) PP: Truncated with thread having flute	Z: NA	
		T: NA	
		F: NA	
You et al. [110]			1. Welding torque significantly reduces by increasing welding speed, which is highly suited for robotic manufacturing.
AA2219-T6	a) 14/8	N$_P$: 2000-2600	
H: 4	b) 8/5/4/3.9	V: 100	2.Enhanced mixing of materials occurs in the SZ by increasing tool rotational speeds
TM: NA	c) PP: Conical threaded pin	Z: NA	
		T: NA	

Table 4. Continued…

Authors	NRSA-FSW tool geometry	FSW process parameters	Remarkable effects of NRSA-FSW
Alloy, Tool Material	a) NRS-OD/ID		
	b) RTS-SD/PTD/PBD/PL		
	c) PP		
		F: NA	
Ji et al. [111]			
AA6005-T6	a) 12/6.3	N$_P$: 2000	1. Obtained defect-less joints with smooth weld surface.
H: 4	b) 6/5/NA/3	V: 100-600	
TM: NA	c) PP: Tapered threaded pin	Z: NA	
		T: NA	
		F: NA	
Li et al. [113]			
AA6061-T6	a) 16/NA	N$_P$: 750-1500	1. No visible TMAZ and narrower HAZ.
H: 5	b) NA/8/5/4.9	V: 100-300	
TM: NA	c) PP: Conical threaded pin	Z: NA	
		T: NA	
		F: NA	
Li et al. [122]			
AA2024-T4	a) 17/10.5	N$_P$: 800-1200	1. High rotational speed is required for the adequate vertical displacement of the material in the SZ.
H: 3	b) 10/5/3.5/5	V: 50	
TM: NA	c) PP: Tapered threaded pin	Z: 0.2	
		T: NA	
		F: NA	
Yue et al. [115]			
AA2024-T4	a) 17,21/10.5	N$_P$: 1000	1. High welding speed leads to void formation on the advancing side.
H: 3	b) 10/5/3.5/5	V: 50-200	2. Increase in the diameter of stationary shoulder increases effective sheet thickness and effective lap width.
TM: NA	c) PP: Tapered threaded pin	Z: 0.2	
		T: NA	
		F: NA	
Buffa et al. [123]			
AA6082-T6	a) 9/NA	N$_P$: 2500	1. Obtained high quality surface with no flash defects.
H: 2	b) NA/3/NA/3	V: 480	2. Temperature distribution was found consistent due to stationary shoulder.
TM: NA	c) PP: Conical threaded pin	Z: NA	
		T: NA	
		F: NA	
Chen et al. [114]	a) 11/NA	N$_P$: 1200	1. As compared to traditional FSW, hook defect was eliminated in the joints produced by stationary shoulder.
AA7075-T651	b) NA/5/4/2.75	V: 200	2. Low heat input prevents the coarsening of strengthening precipitates and fracture took place from the zone of kissing bond defect.
H: 5-3	c) PP: NA	Z: 0.25	
TM: NA		T: NA	
		F: NA	

AA: aluminum alloy; NA: Not Available; H: Height of plate in mm; TM: Tool material; NRS: Non-rotational shoulder, OD/ID: Outer and inner diameter in mm; RTS: Rotating shoulder, SD: Shoulder diameter; PTD: Pin top diameter in mm; PBD: Pin bottom diameter in mm; PL: Pin length in mm; PP: Pin profile; N$_P$: Rotational speed of pin in rpm V: Welding speed in mm/min; T: Tool tilt angle in degree; F: Axial force in KN; Z: Plunge depth of NRSA-FSW in mm;

4.2. Counter-rotating twin tool friction stir welding (CRTT-FSW)

In a continuous endeavor to improve FSW joint quality, several tools with different materials and technologies are tried by modification in the existing conventional FSW. Advanced auto-adjustable tool pins are designed to reduce defects such as keyholes or craters in the weld joint [124]. In addition, to enhance the weld joint properties, a twin tool set-up for friction stir welding was fabricated and built by kumari et al. [125], as illustrated in Figure 13a. Twin-tools are made up of two tools, one primary and one secondary, that rotate in opposite directions. During the welding process, the primary tool was mounted on the main spindle shaft and rotated at the same rotational speed and in the same direction as the spindle. The secondary tool was linked to the primary tool via a gear arrangement (see Figure 13b).
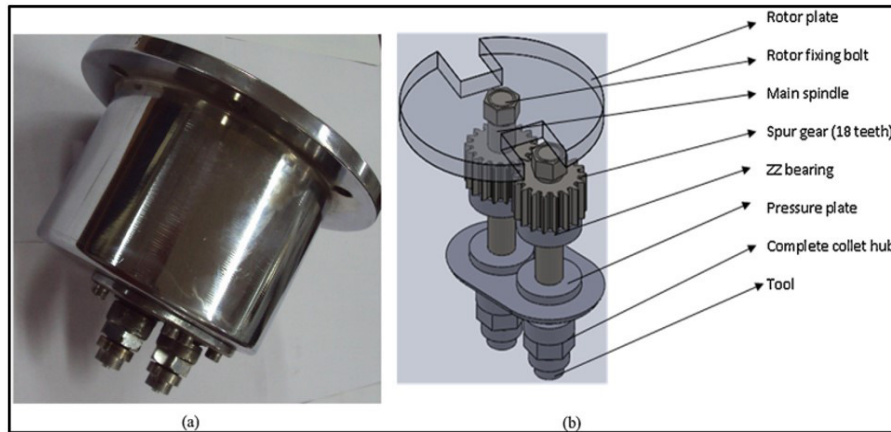

Figure 13. Counter-rotating twin tool set-up (a) schematic diagram (b) [125].

Techniques such as counter-rotating twin tool (CRTT) helps to produce higher frictional heat, which causes severe plastic deformation resulting in a defect-free weld [125]. However, due to higher frictional heat excessive flashes are formed. In addition, the violent stirring effect was achieved by this tool which significantly reduces the inadequate heat input defects such as tunnel defect. Jain et al. [126], reported that as compared to traditional FSW, the flow of material was enhanced during CRTT-FSW. The material from the AS was deposited closer to its initial location for CRTT leading to lower chances of defects in the former [125,126]. The interactive effect of tool rotational and tangential speeds also plays a significant role in attaining defect-free weld joints. But due to the difference in the shoulder and pin tangential speeds, overheating across the edge of the shoulder takes place, and flashes are formed, which deteriorates the mechanical properties of the weld joint [127,128]. Insufficient or inadequate heating leads to cavity and groove defects [129]. The cross-sectional macrograph for insufficient and excessive heat input is shown in Table 5. Overheating leads to the formation of flashes [129,130] which is depicted in figure provided in the Table 5. The CRTT processed specimen's shows enhanced material flow in the SZ which reduces the improper stirring defects as compared to as weld specimens. The remarkable effects of CRTT-FSW are summarized below in Table 6. Still CRTT-FSW is in its initial stage and further researches should be required in this direction to reveal the its significance for other FSW defects originated from inadequate heat input.

Table 5. Insufficient and overheating defects.

Heat input	Type of defect	Material and Process parameter	Cross-sectional macrograph of the weld [129].
Insufficient heat input	Cavity defect	1) Material: ADC12 2) N: 1500 3) V: 500 4) F: 6.9	
Insufficient heat input	Groove-defect	1) Material: ADC12 2) N: 1500 3) V: 750 4) F: 6.9	
Overheating/ Excessive heat input	Rough surface or Flash defect	1) Material: ADC12 2) N: 1500 3) V: 250 4) F: 14.2	

ADC12: Aluminum die casting alloy, N: Tool rotational speed in (rpm), V: Welding speed in (mm/min), F: Force in (KN).

Table 6. Remarkable effects of CRTT-FSW.

Authors	CRTT-FSW tool geometry	FSW process parameters	Remarkable effects of NRSA-FSW
Alloy, Tool Material	a) PiT/SeD		
Kumari et al. [125]	SD(PiT/SeD): 16/16	N_P: 900-1800	1. Enhances the stirring effect of the tool and reduces the tunnel defect to minimum.
AA1100	PL(PiT/SeD):: 2/2	V: 16-63	2. Except flashes the defect-free joints are observed in higher welding and rotational speeds.
H: 2.5	PD: 5	Z: NA	
TM: SS316 steel	PP: cylindrical pin/cylindrical pin	T: NA	
		F: NA	
Jain et al. [126]	SD(PiT/SeD): 16/16	N_P: 900-1800	1. Enhances the flow of material from AS to RS in the SZ.
AA1100	PL(PiT/SeD): 2.6/2.6	V: 16-63	2. Significantly reduces the chances of defects in the former due to enhanced stirring effect of CRTT.
H: 3	PD: 5	Z: 0.1	
TM: H13 steel	PP: cylindrical pin/cylindrical pin	T: 0°	
		F: NA	

AA: aluminum alloy; NA: Not Available; H: Height of plate in mm; TM: Tool material; PiT: Primary tool; SeD: Secondary tool; SD: Shoulder diameter in mm; PD: Pin diameter in mm; Pcs: Cross section of pin in mm; PL: Pin length in mm; PP: Pin profile; N_S: Rotational speed of shoulder in rpm; N_P: Rotational speed of pin in rpm V: Welding speed in mm/min; T: Tool tilt angle in degree; F: Axial force in KN; Z: Plunge depth of reversely rotating assisted shoulder in mm.

4.3. Reverse dual rotational friction stir welding (RDR-FSW)

Reverse dual-rotation friction stir welding (RDR-FSW) is a novel FSW process in which the tool pin and the surrounding assisted shoulder rotate in the opposite direction, which has the potential to improve weld quality and reduce welding loads by independently adjusting the rotating speeds of the tool pin and the assisted shoulder. Hence, the tool shoulder and pin are designed to rotate independently, either in the same or reverse direction to minimize the overheating effect and enhance the tool's stirring action. Figure 14 shows the tool system for the RDR-FSW where the tool and shoulder rotate independently with each other either at different or same rotational speeds with the help of two servo motors. The clamping requirement and the tool torque is reduced due to reverse dual rotation of shoulders (one assisted shoulder) or shoulder and pin which ultimately reduces the mass and size of FSW equipment. The RDR-FSW is beneficial for welding high-strength aluminum alloys because a large amount of plastic deformation occurs at high temperatures due to the intense stirring of tool [131]. Figures 15 and 16 shows the weld surface of CRTT and RDR-FSW. from the figures, it is evident that flash-free weld was obtained by the reverse dual rotational friction stir welding RDR-FSW [132,133].
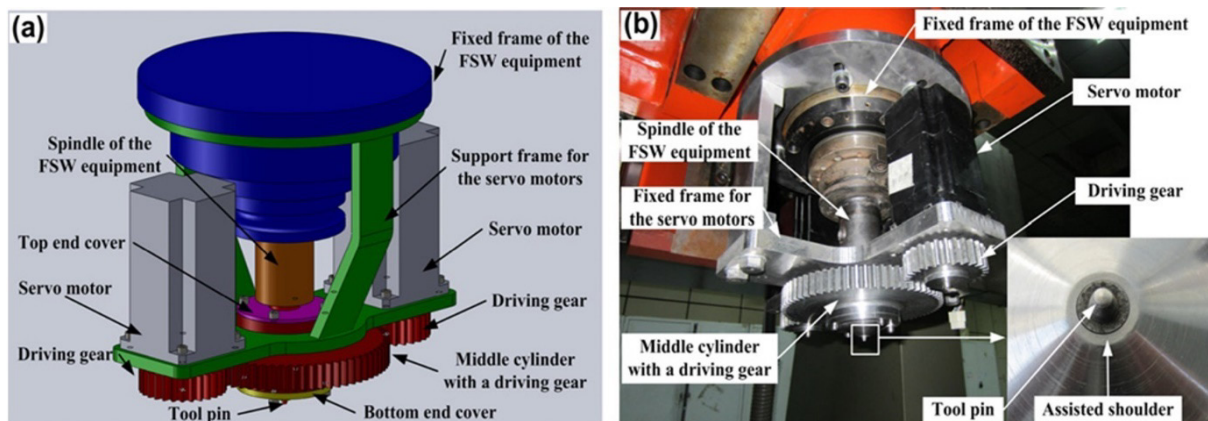

Figure 14. RDR-FSW (a) Schematic view and (b) Tool set-up image [131].

Figure 15. Weld joint obtained from counter-rotating twin tool [125].
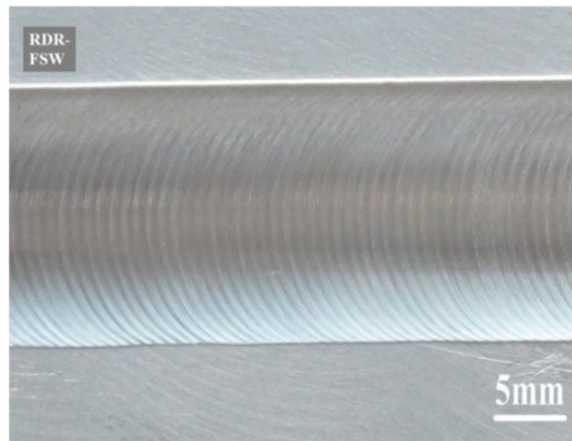
Figure 16. Weld joint obtained from RDR-FSW [132].

Figure 17a and Figure 17b show the weld obtained from the RDR-FSW and conventional FSW process [132]. Figure 17b highlights the undesirable reduction in weld thickness due to severe forging action during welding, where an extra amount of plasticized material is extruded from the retreating side resulting in flash and cavity defects [132,134]. However, in the case of RDR-FSW the reverse rotation of assisted shoulder prevents material from escaping, eliminating thickness reduction and formation of such defects [134].
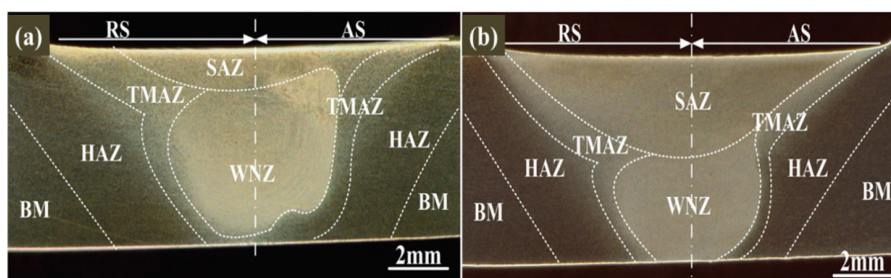
Figure 17. (a) AA2219-T6 weld macrograph of RDR-FSW (b) Macrograph of conventional FSW at 1800 rpm tool rotation and 200 mm/min welding speed.(AS: advancing side, RS: retreating side, BM: base metal, HAZ: heat affected zone, TMAZ: thermomechanically affected zone, SAZ: shoulder affected zone, WNZ: weld nugget zone) [132].

Figures 18 and 19 displays the grain structures of RDR-FSW [135] and macroscopic appearances of non-rotational shoulder assisted (NRSA-FSW) [136]. Defect-less welds are obtained in both the welding process. Authors performed welding in a wide range of tool shoulder and pin speeds. NRSA-FSW improves the mechanical properties at a tool shoulder (N_S), and pin (N_P) rotational speed of 800rpm and welding speed of 150-250mm/min. In most of the cases the conical threaded pin profile displays fine grains and improves material flow. However, due to reverse rotation and slower rotational rate of tool shoulder the degree of heat input decreases, which lead to the formation of small cavity defects which can be further eliminated by optimizing the process parameters [134,137]. However, the research regarding this context is very limited, only few authors studied and explained about reduction in total net tool torque [106,138], intermetallic compounds (IMCs) formations at weld nugget during dissimilar joining [139]. Some numerical analysis presented the

significance of material flow and heat transfer [140,141]. Additionally, investigations in this direction is needed to enhance mechanical mixing, bonding, and selection of FSW process parameters.
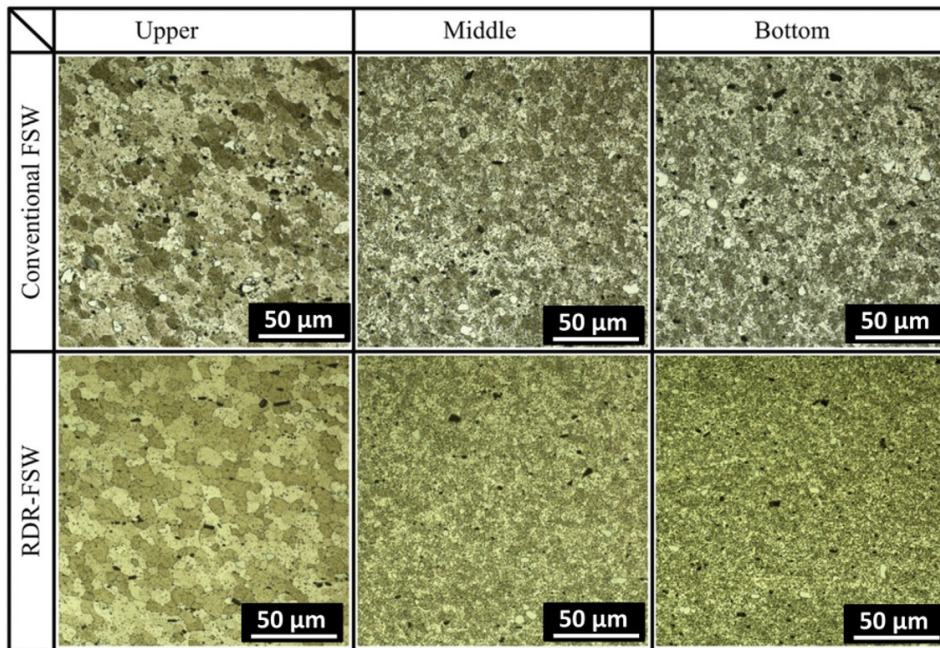
Figure 18. Grain structures of AA2219-T6 weld nugget zone for conventional FSW and RDR-FSW at FSW at 800 rpm tool rotation, 200 mm/min welding speed (for both tool pin and assisted shoulder) and 0.2 mm plunge depth [135].
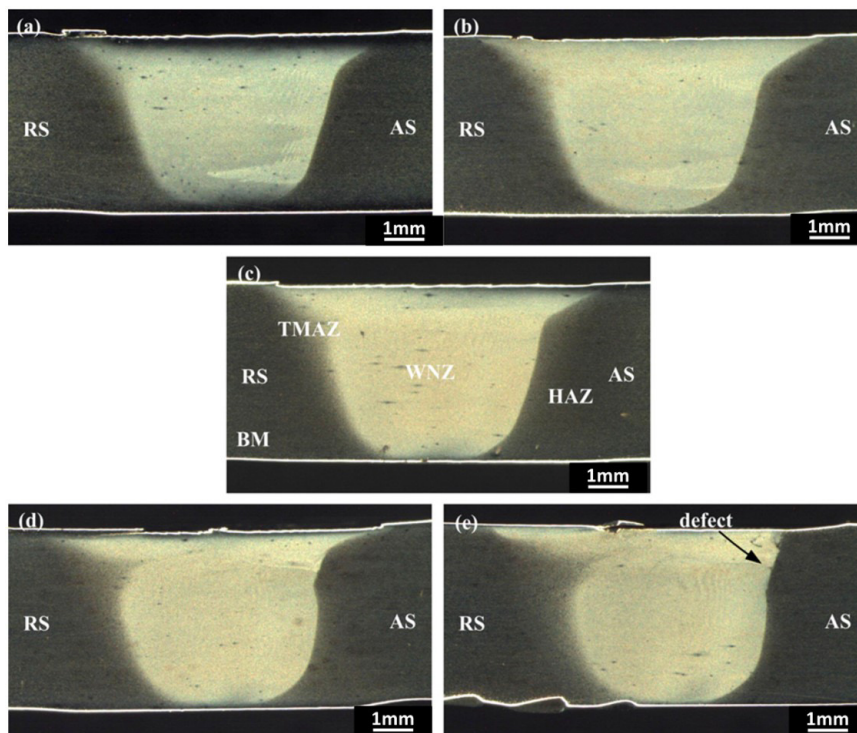
Figure 19. AA2219-T6 weld cross section of non-rotational shoulder assisted NRSA-FSW at constant 100 mm/min welding speed and different tool rotational speeds (a) 600 rpm, (b) 700 rpm, (c) 800 rpm, (d) 900 rpm, (e) 1000 rpm (abbreviations are mentioned in caption of Figure 17) [136].

Li and Liu [131] designed tool for the RDR-FSW and due to reverse rotation of the tool and shoulder, overheating across the shoulder edge reduces and enhances the tool's stirring effect, resulting in defect-free weld. Figure 20 shows the optical macrograph of the stirred zone without any internal defect, welded by RDR tool [131]. Additionally, improvement in tensile

strength is observed compared to without dual rotational FSW. The hardness value decreases towards the weld center, and failure occurs at this region due to larger grain size produced at elevated temperature during intense stirring action of the tool.
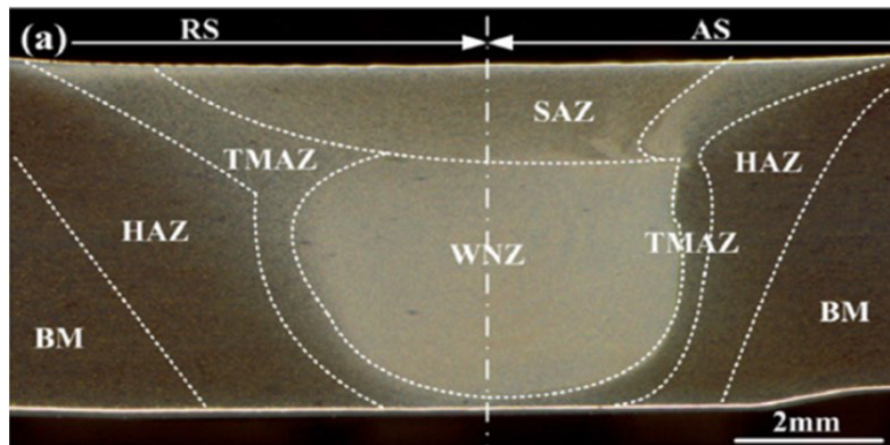
Figure 20. AA2219-T6 weld cross-section of RDR-FSW at 100 mm/min welding speed and 800 rpm rotational speed for both tool pin and reversely rotating shoulder (abbreviations are mentioned in caption of Figure 17) [131].

Li and Liu [135] found that as compared to conventional FSW, the heat input in RDR-FSW considerably reduced during the welding process. The softening of different FSW zones is attributed to the dissolution of strengthening precipitates and coarsening of grains induced by the thermal cycle during the FSW process [142]. The lower heat input in RDR-FSW significantly reduced the weld thermal cycle time, which shows fine and dense precipitates in the HAZ and TMAZ [143] than conventional FSW depicted in Figure 21 and Figure 22. Moreover, at the stirring zone, the formation of equiaxed grains structure and reduction in grain size were observed at the weld nugget zone (WNZ) in RDR-FSW. Li and Liu [138] developed a mathematical model to optimize the process parameters of RDR-FSW. The tensile test results of the weldment reveal that by increasing the tool pin rotational speed and at the same time by decreasing the speed of assisted shoulder (rotating in the reverse direction) the tensile strength of the joint increases by 5.2% as compared to conventional FSW. Mehdi et al. [144] reviewed several mathematical modeling regarding flow patterns of different sections along thickness and reported that the Reverse dual-rotation in FSW shows different flow patterns at different horizontal sections of the plate and also improves the weld joint quality by lowering the tool torque. The remarkable effects of reverse dual rotational FSW are summarized below in Table 7. Reverse dual rotational FSW is considered one of the novel variants of FSW-supporting tool systems [135,146]. By independently adjusting the rotational speed of the pin and assisted shoulder, we can modify the velocity gradient between the shoulder and probe center. Such adjustments lower the welding loads and reduce the tendency towards overheating near the shoulder side [106]. Several studies confirmed that by lowering shoulder rotational speed, the thermal softening effect at heat affected zone reduces, and the weld joint strength improves [144,147]. Moreover, the potential benefits of reverse dual rotational FSW include improvement in joint efficiency, cost reduction, etc. Further, many more alternative tool types could be invented to investigate their motions and effects on weld joint fatigue properties.
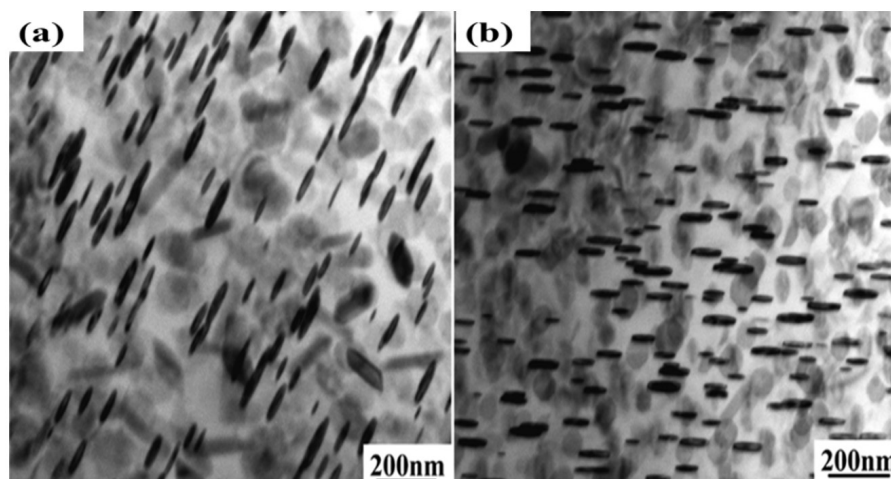
Figure 21. Transmission electron microscopy (TEM) images of HAZ (a) Precipitates of conventional FSW, (b) Precipitates of RDR-FSW [135].
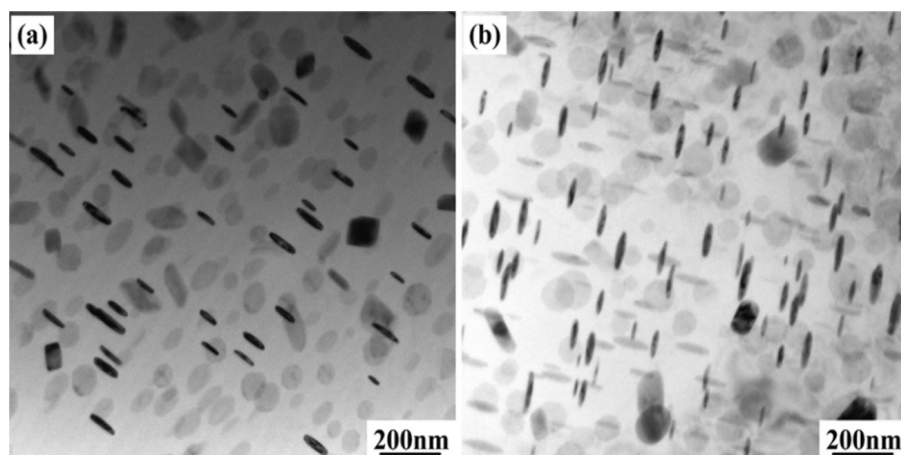
Figure 22. TEM images of precipitates at TMAZ (a) FSW joint (b) RDR-FSW joint [135].

Table 7. Remarkable effects of RDR-FSW.

Authors Alloy, Tool Material	RDR tool geometry	FSW process parameters	Remarkable effects of RDR-FSW
Li and Liu [131]	Assisted SD: 14	N_S: 800	1. Improve tensile strength, and defect-free weld joints are produced due to the extreme stirring action of tool.
AA2219-T6	Mean PD: 4.52	N_P: 800	2. Grain structure becomes more refined and distributed uniformly in the weld nugget.
H: 5	PL: 4.8	V: 150	
TM: NA	PP: Conical threaded pin	Z: 0.2	
		T: 2.5º	
		F: NA	
Li and Liu [135]	Assisted SD: 14	N_S: 800	1. Higher grain refinement was observed at weld nugget, but the grains' size increases towards the heat-affected zone.
AA2219-T6	Mean PD: 4.52	N_P: 800	2. Precipitates are finer in TMAZ and HAZ compared to conventional FSW.
H: 5	PL: 4.8	V: 200	3. Decrease in the plastic flow of material because the flow is constrained below the reversely rotating tool.
TM: NA	PP: Conical threaded pin	Z: 0.2	
		T: 2.5º	
		F: NA	
Li and Liu [138]	Assisted SD: 14	N_S: 200-800	1. Optimized process parameters of welding show better tensile strength than conventional FSW.
AA2219-T6	Mean PD: 4.52	N_P: 200-800	2. Reduction of total welding torque was found due to reverse rotation of shoulder and pin.
H: 5	PL: 4.8	V: 150-250	
TM: NA	PP: Conical threaded pin	Z: 0.2	
		T: 2.5º	
		F: NA	
Jamshidi Aval and Loureiro [139]	Assisted SD: 14	N_S: 600	1. The slower rotational speed of assisted shoulder reduces the amount of intermetallic compounds formed at the weld interface of lap joints.

Table 7. Continued…

Authors	RDR tool geometry	FSW process parameters	Remarkable effects of RDR-FSW
Alloy, Tool Material			
AA7075-T6, AISI304 Stainless steel	PD: 5	N_P: 1000	2. Higher grain refinement is achieved in the nugget zone due to the slower rotational speed of assisted shoulder.
H: 2,1	PL: 2.1	V: 120	
TM: NA	PP: Cylindrical pin	Z: 0.2	
		T: 2.5º	
		F: NA	
Zhou et al. [145]	Assisted SD: 14	N_S: 400-1200	1. By increasing shoulder rotational speed, defect-free joints and enlarged weld zone were attained.
AA6061-T6	PD: 3.45-6.2	N_P: 1200	2. Higher tensile strength and microhardness value was found compared to conventional FSW.
H: 5	(from pin tip to root)	V: 200	
TM: NA	PL: 4.8	Z: 0.1	
	PP: Conical threaded pin	T: 3º	
		F: NA	
Liu et al. [132]	Assisted SD: 14	N_S: 1000	
AA2219-T6	Mean PD: 4.52	N_P: 800	1. The reverse rotation of the tool shoulder and pin reduces the microstructural asymmetry of the weld nugget.
H: 5	PL: 4.8	V: 250	2. Increase in welding efficiency was found due to slower and higher rotational rate of shoulder and pin.
TM: NA	PP: Conical threaded pin	Z: 0.2	
		T: 2.5º	
		F: NA	
Shi et al. [106]	Assisted SD: 14	N_S: 600-800	
AA2024	PD: 4-6	N_P: 800-1200	1. In this numerical analysis non-axisymmetric heat generation rate was found at the shoulder-work piece contact, the peak value of heat generation rate was found maximum in front of the tool.
H: 5	(from pin tip to root)	V: 60-80	2. Decrease in the total net torque value was found due to the reverse rotation of the pin and shoulder.
TM: NA	PL: 4.8	Z: NA	
	PP: Conical threaded pin	T: NA	
		F: NA	

AA: aluminum alloy; NA: Not Available; H: Height of plate in mm; TM: Tool material; SD: Shoulder diameter in mm; PD: Pin diameter in mm; Pcs: Cross section of pin in mm; PL: Pin length in mm; PP: Pin profile; N_S: Rotational speed of shoulder in rpm; N_P: Rotational speed of pin in rpm V: Welding speed in mm/min; T: Tool tilt angle in degree; F: Axial force in KN; Z: Plunge depth of reversely rotating assisted shoulder in mm.

4.4. Self-Reacting/Support Friction Stir Welding (SRFSW)

FSW has a wide range of applications in industrial and engineering fields [148], mainly used for welding ductile materials such as aluminum and magnesium alloys [149-151]. However, the application of this technique is limited for very hard and thick materials because a substantial amount of plunge force is required during tool pin insertion and shoulder contact, which deteriorates its axial rigidity [152,153]. To overcome the instability of the tool during welding thick plates, a new tool known as self-reacting/double sided/bobbin tool (SR-FSW) has been developed. SR-FSW minimizes the need of backing plate and this unit is capable to adjust the processing load itself [104,154,155].

The defect, such as lack of penetration (LOP) and root flaws in the lower surface of conventional FSW joint, initiate the formation of kissing bonds as shown in Figure 23a, b and c. This in turn reduces the fatigue life, strength and other properties of

weld joint [158,159]. To eliminate these defects, the SR-FSW technique is employed [160]. However, it was observed that this bond and root overlap is formed and shifted to the middle layer of the nugget zone towards the pin end during SR-FSW [161,162]. Also, due to the asymmetrical arrangement of the tool, the upper and lower tool pin mismatch occurs at the stir zone leading to the formation of the tunnel, S-line, and flash defect [157,163,164] depicted in the Figure 23d. The formation of such bonds could be eliminated using bobbin tool by further optimizing the FSW process parameters [165,166].
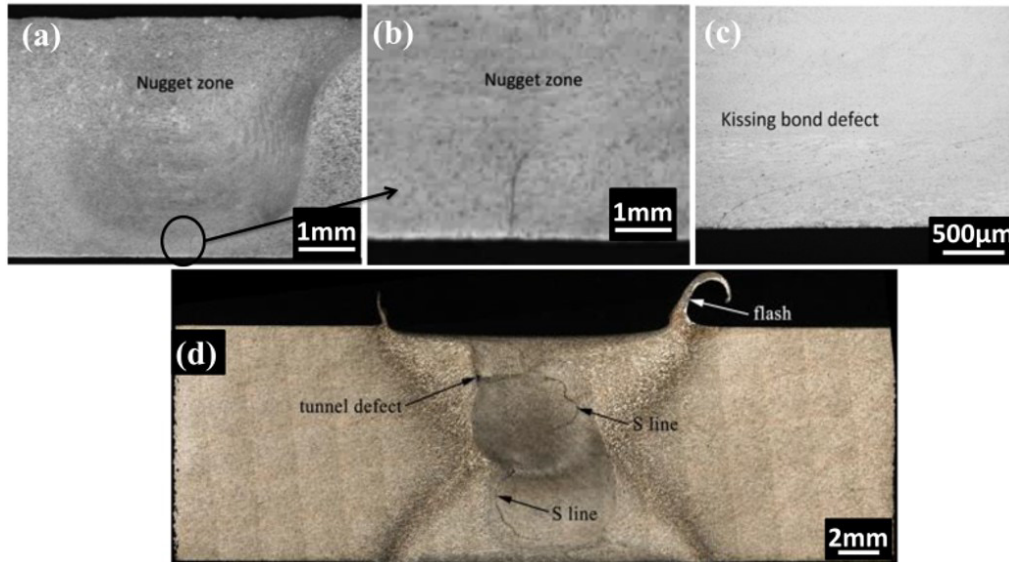
Figure 23. AA7475-T7351 weld cross-section showing defects formation in conventional FSW(a, b) Lack of penetration at 300 rpm rotational speed (N) and 150 mm/min welding speed (V) [156] (c) Kissing bond at N of 500 rpm and V of 400 mm/min [156] (d) AA7085-T7452 weld cross-section showing tunnel, S-line and flash defect formation in Double Sided FSW at N of 950 rpm and V of 60 mm/min [157].

The bobbin tool friction stir welding technique, also known as self-reacting/support friction stir welding (SRFSW) technique in which purposely designed tool composed of the upper shoulder, lower shoulder and a pin in between both the shoulders is used for friction stir welding process. The upper and lower shoulder gap called pinching gap is maintained by turning the lower shoulder which is fixed on the nut [167] as shown in the Figure 24. However to enhance the stirring effect, several other kinds of pin designs like cylindrical threaded pin, cylindrical pin with grooves, cylindrical 4 flats pin (square pin) can also be preferred in SRFSW [168].
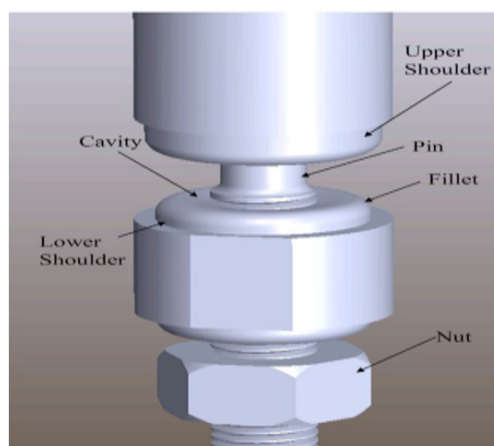
Figure 24. SRFSW tool [167].

Sued et al. [168] designed threaded, grooved and flat types of tool pin profiles and found that the cylindrical 4 flat (square) pins profile as shown in Figure 25 produced sound weld joint. Additionally, the essential compression effect can be achieved during welding since the distance between shoulders can be adjusted according to the thickness of the plate to be welded. At the same time the arrangements like support and clamp act as a heat-sink that dispels heat. Huang et al. [169] designed a novel bobbin tool with adjustable dip having concave upper and convex lower shoulders that produces uniform weld ripples and

eliminates the root flaws formed in conventional FSW. Hou et al. [170] investigated the effect of shoulder size on weld joint properties, and it was found that the small shoulder size compared to upper shoulder produces groove defect with excessive flashes along the weld line and, this defect reduces with increasing lower shoulder diameter.

Figure 25. Cylindrical 4 Flat (square) pin profile [168].

Okamoto et al. [171] demonstrated the effect of the shoulder pinching gap at the center and periphery of the self-designed threaded pin with three flats having a convex scroll type of shoulder configuration, as shown in Figure 26. In this study, it was found that small gaps produce defect-free weld joints. In addition, the natural oxide layer present at the pre-weld surface and lower surface kissing bonds along joint was completely eliminated after welding due to scrolled shoulder configuration of bobbin tool FSW.
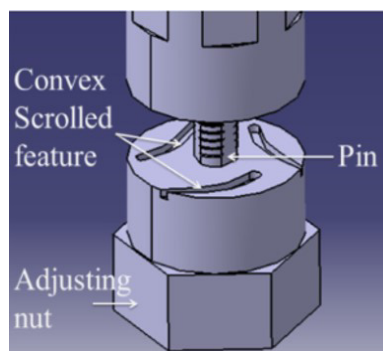
Figure 26. Schematic diagram of bobbin tool having the convex scrolled feature.

Zhang et al. [165] demonstrated the importance of tool pin profile to achieve proper and smooth stirring effect in SRFSW process. In this study, the author used a flat type of pin profile with a concave scrolled feature in the welding process, as shown in Figure 27. It was reported that the improper stirring effect in the middle layer of the weld nugget at lower welding speed forms the ellipse-shaped region, and triangular shaped region towards AS as depicted in the Figure 28. However, by increasing the welding speed ellipse-shaped region starts mixing in the stirred zone as well as triangular shaped region decreases but voids are formed due to improper stirring effect of tool which can be further optimize by using different type of tool pin profile.
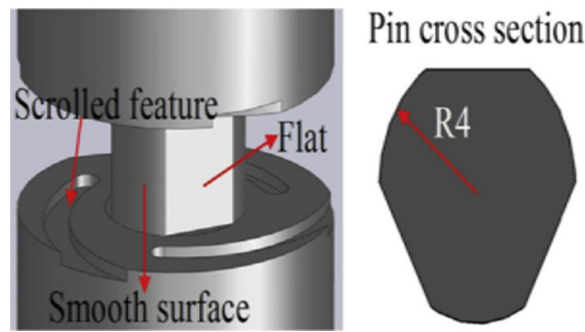
Figure 27. Geometry of the bobbin tool having concave scrolled feature [165].
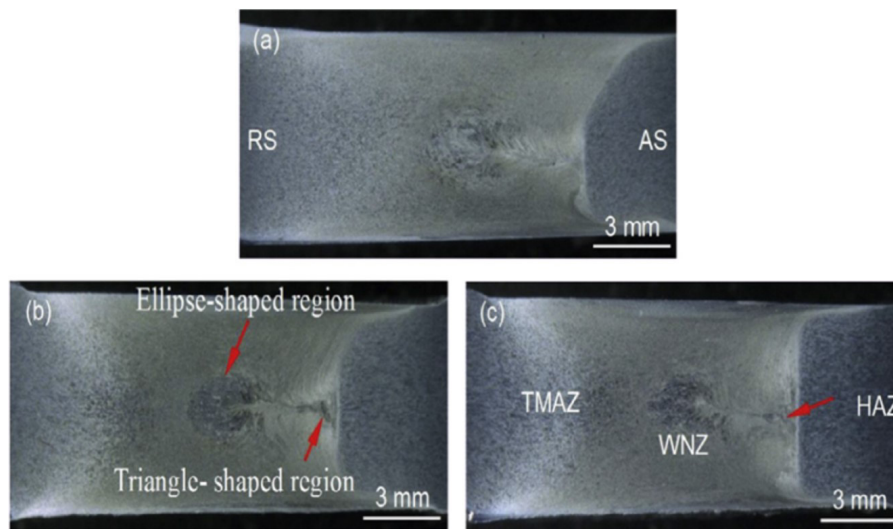
Figure 28. Macrographs of AA2A14-T6 showing formation of ellipse and triangular shaped region in the middle layer of NZ at constant 400 rpm tool rotation and at different welding speeds (V): (a) V=50 mm/min, (b) V=100 mm/min, (c) V=150 mm/min [165].

Wan et al. [172] reported that the welding speed plays vital role in altering mechanical and microstructural properties of joints prepared by SRFSW process. Hourglass-shaped WNZ are formed because the material flow of the upper and lower layers experience higher frictional heat, which softens the material around the pin, upper and lower shoulders depicted in Figure 29. Furthermore, the test result shows that the joint properties such as microhardness value, tensile strength are enhanced and the defects such as tunnel, band defects are eliminated by increasing the welding speed as shown in Figure 30.
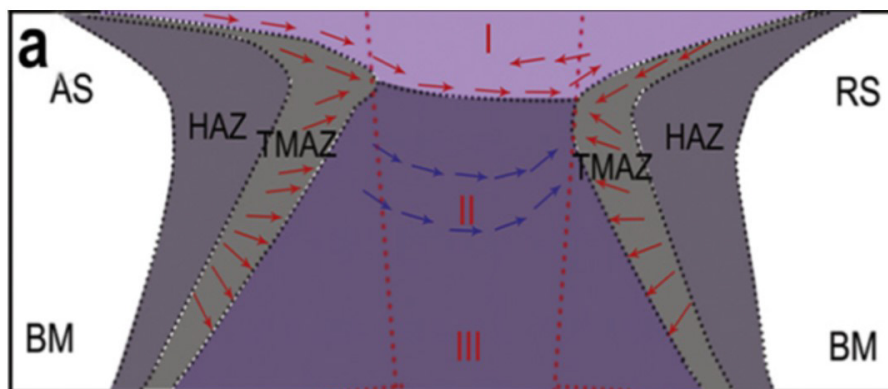
Figure 29. Schematic representation of material flow around SRFSW tool [172].
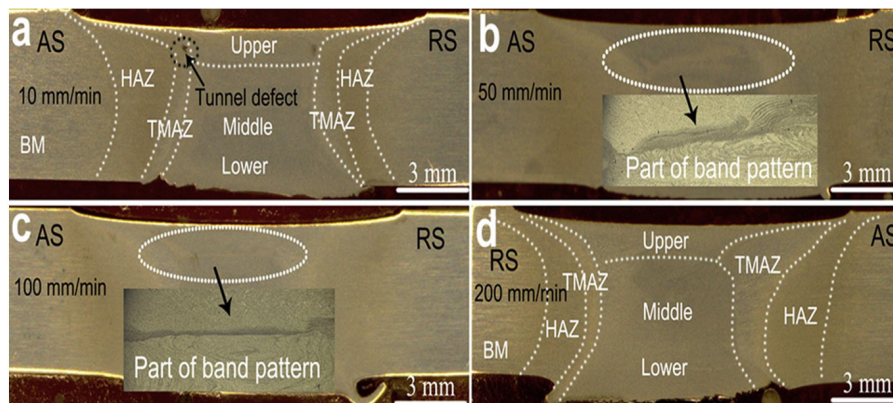
Figure 30. AA6082-T6 macrographs of transverse cross-sections welded by Self-reacting tool at constant tool rotation of 800 rpm and welding speeds of (a)10 , (b) 50, (c) 100 and (d) 200mm/min (AS: advancing side, RS: retreating side, BM: base metal, HAZ: heat affected zone, TMAZ: thermomechanically affected zone) [172].

Wang et al. [173] improved the weld formability by using novel bobbin tool having different upper and lower shoulder speed. In this study authors reported that the dual rotation bobbin tool FSW (DBT-FSW) showed excellent process stability and capable of producing defect free joints at wide range of welding speeds. Moreover, improvement in material flow was observed due to dual rotation depicted in Figure 31, which eliminates the cavity defects formed in conventional bobbin tool FSW (BT-FSW). The remarkable effects of bobbin tool FSW is summarized below in Table 8. The bobbin or self-reacting tool is another important FSW supporting tool system that is generally used to eliminate root defects, partial penetration or lack of penetration formed in conventional FSW [179,180]. This technique's operating temperature is higher than the conventional FSW process due to the absence of backing plate, which dispels heat during the welding process. The elevated operating temperatures can be controlled by reducing the lower shoulder diameters resulting in lower frictional resistance, hence less bending moment and torque on tool [181]. To attain maximum possible benefit of higher operating temperature the tool design and welding parameters need to be adjusted properly [104,148]. The convex scrolled feature on shoulder of bobbin tool enhances the material flow [173], towards tool pin and eliminates the requirement of tool tilting [165].
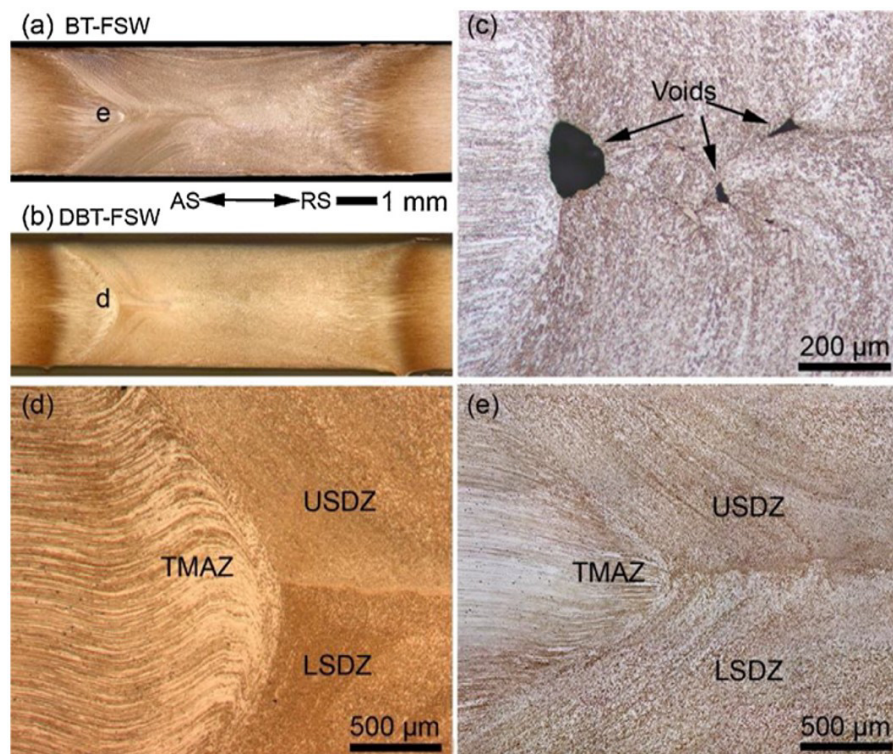
Figure 31. Optical macrographs of AA2198-T851 for a) Conventional bobbin tool FSW (BT-FSW) and b) Dual rotation bobbin tool FSW (DBT-FSW). c) Typical void formation in BT-FSW. d) Advancing side of BT-FSW and e) DBT-FSW where USDZ is upper shoulder dominated zone and LSDZ is lower shoulder dominated zone (AS: advancing side, RS: retreating side, TMAZ: thermomechanically affected zone) [173].

Table 8. Remarkable effects of SRFSW.

| Authors / Alloy, Tool Material	SRFSW tool geometry	FSW process parameters	Remarkable effects of SRFSW
Liu et al. [167] AA6061-T6 H: 4 TM: NA	USD: 18 LSD: 16 PD: 8 PL: NA PP: Cylindrical pin	N: 600 V: 50-200 Z: 0.1 T: NA F: NA	1. By increasing welding speed, defects such as band pattern reduce and improve weld joint tensile strength. 2. The tensile strength of defect-free weld joint with increase in welding speed reaches equivalent to 69% of base metal.
Sued et al. [168] AA6061-T6 H: 4 TM: NA	USD (scrolled): 8 LSD (scrolled): 8 PD: NA PL: NA PP: Cylindrical threaded, threaded with 3flat, threaded with 4 flat, 4 sided flat square pin	N: 700 V: 80 Z: 0.1 T: NA F: NA	1. The effect of different pin profiles were studied and sound weld was found in case of 4 sided flat square pin. 2. Essential compression effect during welding was produced by using this tool which increases hardness with decrease in tensile strength of weld joint towards clamp side.
Wan et al. [174] AA6082-T6 H: 5 TM: High speed steel	USD: 14 LSD: 9 PD: NA PL: 4.6 PP: Conical threaded pin	N: 800 V: 50-200 Z: 0.1 T: 4º F: NA	1. Grain refinement takes place in upper and lower layer of weld joint, because of over aging effect and coarser second phase particles. 2. Hourglass-shaped weld were attained using this tool with no obvious change in grain structure and size compared to base metals in HAZ.
Esmaily et al. [166] AA6005-T6 H: 10 TM: NA	USD: 24 LSD: 24 PD: 8-10 (from pin tip to root) PL: 9.8 PP: Tri flat conical threaded pin	N: 500-1200 V: 500-1200 Z: 0.1 T: 2º F: NA	1. Formations of kissing bonds take place at the lower weld surface of conventional FSW which are minimized by using bobbin tool. 2. Heat generation is higher due to which grain refinement takes place from SZ to AS in bobbin tool assisted FSW.
Wan et al. [172] AA6082-T6 H: 5 TM: NA	USD: 14 LSD: 9 PD: NA PL: 4.6 PP: Conical threaded pin	N: 800 V: 10-200 Z: 0.1 T: 4º F: NA	1. Welding speed is a key parameter for enhancing the weld joint quality because at lower welding speeds the band pattern and series of onion rings are formed which can be eliminated by optimizing the welding speed. 2. Increase in welding speed reduces the tunnel defect as well as enhances the tensile strength of weld joint.
Hou et al. [170] AA6061-T6 H: 4 TM: NA	USD: 18 LSD: 16, 14, 12 PD: 8 PL: NA PP: Cylindrical pin	N: 400-800 V: 150 Z: 0.06 T: NA F: NA	1. Increasing the difference in upper and lower shoulder size bring about defects. 2. Voids are formed towards AS of the weld joint. Such defects were eliminated by reducing the rotational speed of tool.
Okamoto et al. [171] AA6082-T6, 6068-T6, 6061-T6, A6N01-T5 H: 5.95 TM: Tool steel	USD: 20 LSD: 20 PD: 10 PL: NA PP: Threaded pin with 3 flats having convex scroll shoulder	N: 600-1000 V: 30-1000 Z: 0.1 T: NA F: NA	1. By decreasing the pinching gap between shoulders enhances the weld joint quality. 2. The oxide remnant so called "lazy S" was eliminated by using convex scroll shoulder shaped bobbin tool.
Zhang et al. [165] 2A14-T6	USD: 16 LSD: 16	N: 400 V: 25-150	1. The scrolled shaped shoulder enhances the material flow and eliminates the requirement of tool tilting. 2. The FSW parameters must be optimized first in order to reduce the formation of ellipse and triangular shaped region.

Table 8. Continued…

Authors / Alloy, Tool Material	SRFSW tool geometry	FSW process parameters	Remarkable effects of SRFSW
H: 6	PD: 8	Z: 0.07	
TM: NA	PL: NA	T: NA	
	PP: Tri flat cylindrical pin (scrolled shoulder)	F: NA	
Zhou et al. [153]	USD: 18	N: 400	1. Defects like flashes and pores are formed at higher and lower welding speeds.
AA6061-T6	LSD: 16	V: 150-450	2. Tensile properties of weld joint increases as well as refined grains are achieved at higher welding speed.
H: 5	PD: 8	Z: 0.1	
TM: NA	PL: NA	T: NA	
	PP: Tetra flat cylindrical pin	F: NA	
Zhao et al. [175]	USD: 16	N: 1200	1. In situ water mist was sprayed to the leading edge of top shoulder which reduces the peak temperature as well as enhances the weld joint properties.
AA6063-T6	LSD: 16	V: 200	2. Defect free joint and 11.4% increase in tensile strength was found in water cooling specimen as compared to as welded specimens.
H: 4	PD: 8	Z: 0.05	
TM: NA	PL: 4	T: NA	
	PP: Threaded cylindrical pin (spiral groove shoulder)	F: NA	
Yang et al. [176]	USD: 22	N: 300, 400, 600	1. Compared to normal FSW, in bobbin tool FSW the weld joint quality is independent of tool rotational speed.
AA6061-T4	LSD: 22	V: 50, 100, 150, 300	2. Weld nugget grains become more refined with increase in welding speed in both the conditions.
H: 6.35	PD: 8	Z: NA	
TM: NA	PL: 6	T: NA	
	PP: Threaded cylindrical pin (scrolled groove shoulder)	F: NA	
Wang et al. [173]	USD: 11	N: 400-1200	1. Bobbin FSW shows higher stability throughout the process as well as defect free joints can also be produced in a wider range of welding parameters.
AA2198-T851	LSD: 11	V: 42	2. The unbalanced forces at upper and lower surface enhance the material flow and eliminate weld defects such as voids.
H: 3.2	PD: 4	Z: 0.1	
TM: NA	PL: NA	T: NA	
	PP: Cylindrical pin	F: NA	
Li et al. [177]	USD: 24	N: 350	1. Increase in welding speeds avoids the tunnel defect. However, at extreme welding speed the weld joint remnants provide an easier path for crack initiation leads to reduction of weld strength.
AA2219-T87	LSD: 24	V: 250-450	2. Improper heat dissipation through bottom shoulder increases the lower surface average grain size of weld nugget
H: 8	PD: 12	Z: 0.1	
TM: NA	PL: NA	T: NA	
	PP: Cylindrical pin (Cavity feature in shoulders)	F: NA	
Goebel et al. [178]	USD: 15	N: 400, 600	1. A tool with one stationary and other rotating shoulder was used and defect less weld with high surface finish were attained on the stationary side of tool.
AA2198-T851	LSD: 15	V: 200, 500	2. High quality weld joints are achieved having hardness and ultimate tensile strength efficiency of 77%^ and 82%.
H: 3	PD: 7	Z: NA	
TM: Pin-MP159, shoulder-X38CrMoV5-1	PL: NA	T: NA	
	PP: Cylindrical pin (Scrolled shoulder)	F: 2.5, 4, 5	

AA: aluminum alloy; NA: Not Available; H: Height of plate in mm; TM: Tool material; USD: Upper shoulder diameter in mm; LSD: Lower shoulder diameter in mm; PD: Pin diameter in mm; Pcs: Cross section of pin in mm; PL: Pin length in mm; PP: Pin profile; N: Tool rotational speed in rpm; V: Welding speed in mm/min; Z: Shoulder plunge depth in mm; T: Tool tilt angle in degree; F: Axial force in KN.

4.5. In-Situ Rolling FSW (IRFSW)

FSW causes some common surface defects like flash, pin holes, voids, and grooves, which reduce the quality of the weld joint. These defects ultimately restricts its application in industrial fields [182,183]. Several surface improvement techniques were

developed such as surface nano-crystallization (SNC) [184], surface mechanical attrition treatment (SMAT) [185] for refining the surface grain size and low plasticity burnishing (LPB) [186]. In such techniques compressive stress is applied directly on the surface to eliminate salt pit corrosion, which enhances fatigue life of material. To improve the quality of the weld surface in FSW a specifically designed tool is used with lubricated roller balls which are fastened to the spherical grooves by brazing. These balls were fixed to the tool which moves independently to the tool shoulder as shown in the Figure 32. In situ rolling friction stir welding (IRFSW) is the surface strengthening technology where low temperature multiple burnishing action is performed to reduce the flash defect and residual stress in the upper surface of the friction stir welded samples [188]. The compression of surface eliminate the pitting corrosion, improves the surface appearance and fatigue life of a component [189,190].
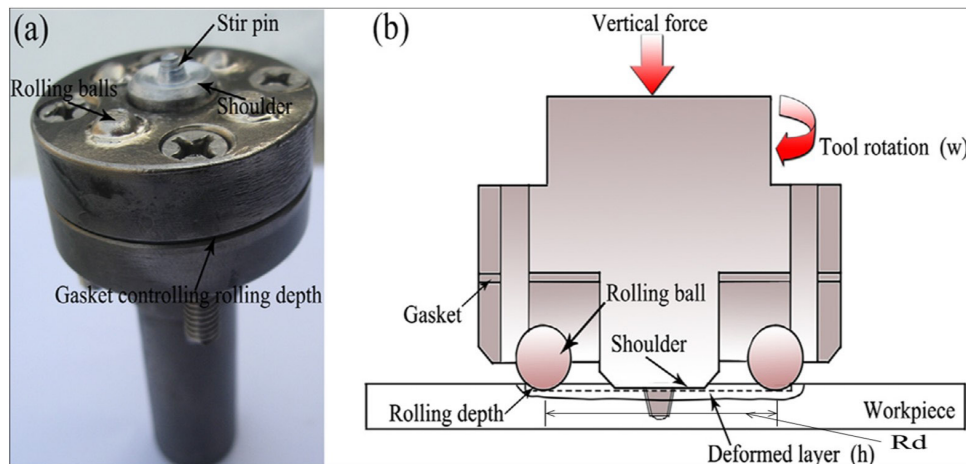

Figure 32. (a) IRFSW tool (b) Schematic illustrations of IRFSW tool, Rd is the rolling diameter of steel balls [187].

Huang et al. [187] studied the surface layer of aluminum alloy welded by in situ rolling FSW tool and found that the micro-hardness of the upper surface layers of the IRFSW-processed samples shows 11.2% increase in hardness value. Additionally, its value decreases towards the lower layers nevertheless tensile strength at optimized parameters increase by 13% compared to base metal. The surface texture at different rolling depth and hardness value of individual layers of welded sample is shown in the Figures 33 and 34.

Huang et al. [105] reported that In-situ rolling tool as compared to conventional FSW tool improve the joint quality to a great extent. Moreover, the rolling effect is advantageous to decrease the residual stress and distortion during welding. The IRFSW tool removes the weld flashes, warm holes at optimized parameters, and smoothens the surface as shown in Figure 35. Huang et al. [191] studied the effect of this new technique on residual stress and distortion of weld joint, and found that In-situ rolling of friction stir weld joints eliminates the flash defects, reduces the residual stress and distortion of weld joints. Furthermore, the in situ rolling processed specimen's shows higher corrosion resistance as compared to as weld specimens. The remarkable effects of in- situ rolling FSW is summarized below in Table 9. To improve the global properties of material, in situ rolling of FSW is considered as the effective alternative without changing its chemical composition [191]. This technique has great potential for reducing weld flashes defects by applying extrusion pressure in AS and RS of weld joint. Also, it reduces the weld residual stress and distortion [189,193]. Thus, this new technique is highly desirable in industrial applications such as large integrally stiffened panels of airplanes, due to its simplicity and flexibility in nature [195]. Thus, from the various literatures reported it can be concluded that FSW assisted with various supporting tool systems plays a significant role in reduction of defect formation.
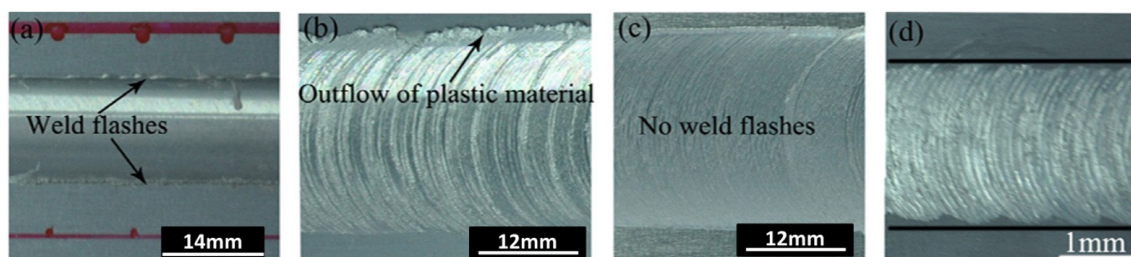
Figure 33. Surface texture comparison of AAA2219 between conventional FSW and IRFSW processed samples at constant 600 rpm tool rotation and 300 mm/min welding speed (a) surface of conventional FSW samples (b) IRFSW with more than 0.05mm rolling depth (c) IRFSW with 0.05mm rolling depth (d) IRFSW with less than 0.05mm rolling depth [187].
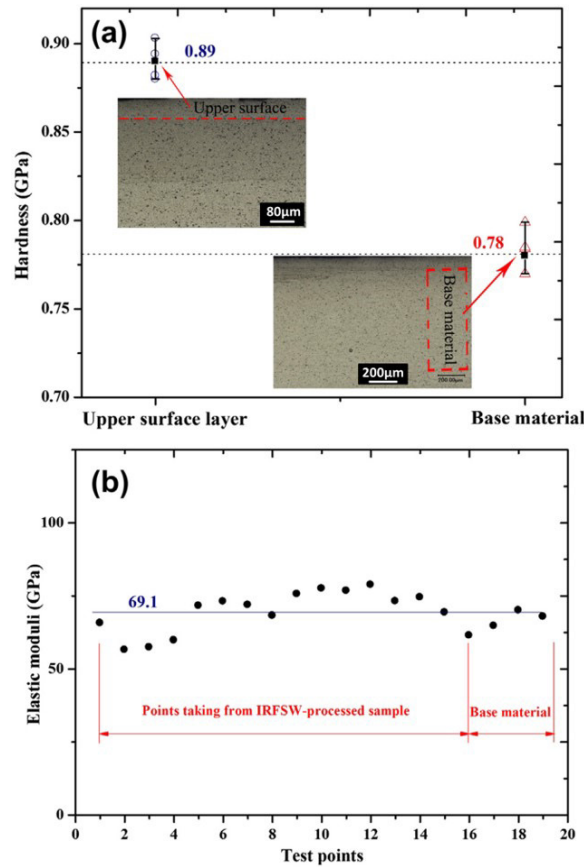
Figure 34. (a) Hardness and (b) Elastic Moduli comparison between base metal and IRFSW processed sample [187].
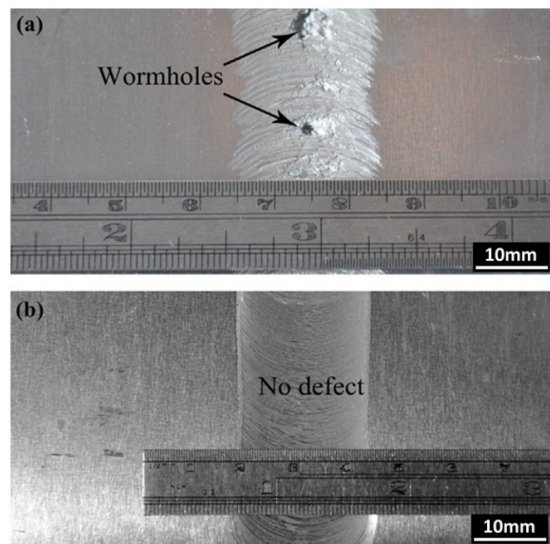
Figure 35. AA2219 weld surface appearance of IRFSW at constant 600 rpm tool rotation and different welding speeds (a) IRFSW with high welding speed (500 mm/min) (b) IRFSW with optimized welding speed (300 mm/min) [105].

Table 9. Remarkable effects of IRFSW.

Authors	In-Situ rolling tool/FSW tool geometry	FSW process parameters	Remarkable effects of IRFSW
Alloy, Tool Material			
Huang et al. [187]	Roller Type: Ball	N: 600	
AA2219	D_B: 8, R_D: 0.05	V: 300	
H: 3mm	SD: 14mm	Z: 0.1	1. Low temperature rolling of upper surface improves the hardness value of upper surface as well as tensile strength of weld joint.
TM: Tool steel	PD: 2.6mm	T: NA	
	PL: NA	F: NA	
	PP: Threaded conical pin		

Table 9. Continued…

Authors / Alloy, Tool Material	In-Situ rolling tool/FSW tool geometry	FSW process parameters	Remarkable effects of IRFSW
Huang et al. [105]	Roller Type: Ball	N: 600	1. Incorporation of rolling tool eliminates flash defects and enhances mechanical properties of weld joint.
AA2219	D_B: 8, R_D: 0.05	V: 100-500	2. Percentage increase in Tensile strength and hardness value is 13% and 20%
H: 3mm	SD: 14mm	Z: 0.1	
TM: Tool steel	PD: 2.6mm	T: NA	
	PL: NA	F: NA	
	PP: Threaded conical pin		
Hassanifard et al. [192]	Roller Type: Ball	N: 1400	1. In situ rolling of smaller and larger rolling balls enhances the weld strength of joint by 25 and 40% as compared to conventional FSW process.
AA6061-T6	D_B: 6,8, R_D: 0.05-0.7	V: 36	2. grains becomes more refined and uniform especially in heat affected zone as well as improves the fatigue life of the weld joint compared with those of as welded samples.
H: 5mm	SD: 18mm	Z: 1	
TM: NA	PD: 6mm	T: NA	
	PL: 2.6	F: NA	
	PP: Conical pin		
Du et al. [190]	Roller Type: Cylindrical	N: 1200	1. The double sided friction stir welded sample of 6mm thickness was rolled to 4, 3, and 2 mm thickness due to which it improves dislocation density in stirred zone.
AA6061-T6	D_R: NA, W_R: NA	V: 500	2. All the strengthening effect such as solid solution strengthening, precipitating strengthening and grain refine strengthening were stronger than base metals.
H: 6	R_D: 2,3,4, F_R: NA	Z: NA	
TM: NA	SD: NA	T: NA	
	PD: NA	F: NA	
	PL: 4.3		
	PP: Threaded conical pin		
Altenkirch et al. [193]	Roller Type: Cylindrical	N: 800	
AA2024-T3, AA2199-T8	D_R: 100, W_R: 29	V: 200-400	1. Author suggests that the post weld roller tensioning is the cheapest method of reducing the residual stress with lesser force requirement. Moreover, a load of 20 KN is sufficient for reversing the sign of residual stress.
H: 5	R_D: NA, F_R: 10,20,30,40	Z: NA	
TM: MP156	SD: 13	T: NA	
	PD: 5	F: 1.3	
	PL: 4.35		
	PP: Threaded pin		
Huang et al. [191]	Roller Type: Ball	N: 800	1. The rolling tool pressure smoothen the weld surface asperities as well as reduces excessive flash formation.
AA2219	D_B: 8, R_D: 0.05	V: 200	2. As compared to conventional FSW, this new technique reduces the residual stress and enhances the resistance to corrosion.
H: 3	SD: 14	Z: NA	
TM: Tool steel	PD: NA	T: 2.5º	
	PL: 2.6	F: NA	
	PP: Conical threaded pin		
Ghisvand et al. [194]	Roller Type: Cylindrical	N: 500	
304 stainless steel,	D_R: 30, W_R: 10-30	V: 101.6	1. Author investigated the role of direct and indirect rolling of FSW joints and found that at optimized width of roller (equal to tool diameter 20mm) the maximum tensile residual stress reduces by 57.3% for indirect rolling and 97.4% for direct rolling.
H: 3.18	R_D: NA, F_R: 2.5-12.5	Z: NA	
TM: NA	SD: 19.05	T: NA	
	PD: 6.35	F: 31.138	
	PL: 3		
	PP: NA		
Wen et al. [195]	Roller Type: Cylindrical	N: NA	
AA2024-T3	D_R: 100, W_R: 20	V: 300	1. Finite element analysis was carried out to understand the reduction in residual stress induced by FSW, for three rolling methods i.e. in situ roller tensioning (ISRT), in situ direct rolling (ISDR), post weld direct rolling (PWDR). Of the three methods the PWDR showed a significant reduction of longitudinal residual stress as well as distortion of weld joints at similar roller forces.
H: 3.2	R_D: NA, F_R: 10-68	Z: NA	
TM: NA	SD: 18	T: NA	
	PD: 2-4	F: NA	
	(from pin tip to root)		
	PL: 3.2		
	PP: Conical pin		

AA: aluminum alloy; NA: Not Available; H: Height of plate in mm; TM: Tool material; SD: Shoulder diameter in mm; PD: Pin diameter in mm; Pcs: Cross section of pin in mm; PL: Pin length in mm; PP: Pin profile; N: Tool rotational speed in rpm; V: Welding speed in mm/min; Z: Shoulder plunge depth in mm; T: Tool tilt angle in degree; F: Axial force in KN; D_B: Diameter of rolling balls in mm; D_R: Diameter of roller in mm; W_R: Width of roller in mm; R_D: Rolling depth in mm; F_R: Force on roller in KN.

5. Discussions and Future Outlook

The imperfections in a weldment compromise its utility to a great extent and significantly affect the weld joint's overall performance [90]. To eliminate defects and flaws of weld joint the emerging tools and technologies are being utilized in FSW where bonding is obtained in the plastic state due to stirring action of FSW tool [105,196]. Figure 36 highlights the type of defects which can be reduced or eliminated by using various supporting tools and technologies with FSW.

Over the past 15 years there has been remarkable degree of improvement in developing FSW supporting tool systems and differentiating them further from conventional FSW techniques. Various new FSW variants has been developed including preheating technologies, friction stir processing, friction stir spot welding, friction stir knead welding and riveting these specific techniques have their own limitations and advantages. This evolution of FSW has led the process a key competitor to the research on FSW assisted with various tool systems. FSW supporting tools and techniques described above are very useful to enhance the stirring effect and to obtain defect-less joints. A few particular issues are mainly focused on in this current research, such as the effect of FSW assisted tool systems, the influence of FSW process parameters, and tool pin profile on macro and microstructural evolution of friction stir weld joint. Effect of process parameters and tool pin profile on weld joint quality for various FSW assisted tool systems are mentioned in the Table 10. This survey provides researchers with collective information in one research work that highlights the defect minimization techniques and provides a basis for future researchers to take reference.
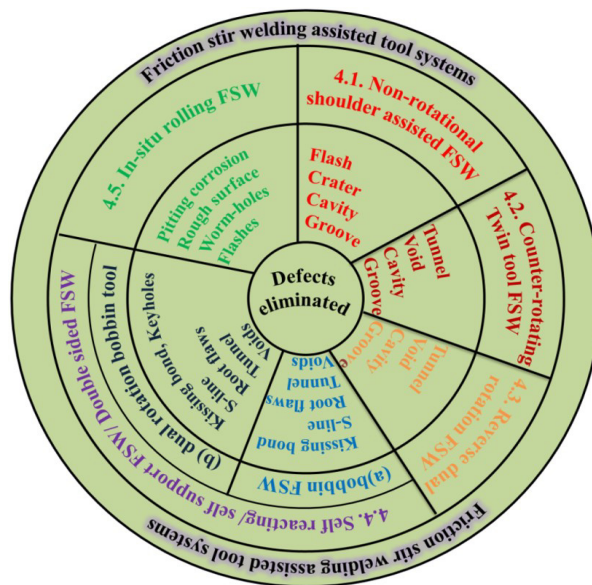

Figure 36. Types of defects which can be rectified or eliminated with the various FSW assisted tool systems.

Table 10. Effect of process parameters and tool pin profile on weld joint quality for various FSW assisted tool systems.

FSW assisted tool systems	Effect of FSW process parameters and pin profile on weld quality
Non rotational shoulder assisted FSW (NRSA-FSW)	The static shoulder designed in NRSA-FSW is used for minimizing overheating defect such as flashes. Conical/tapered threaded pin profile produces defect-less joint with smooth weld surface. Since the shoulder is stationary higher tool pin rotational speed was preferable to generate sufficient heat input for producing the defect-less joints.
Counter rotating twin tool FSW (CRTT-FSW)	Since this variant (CRTT-FSW) is in initial stage and only few literatures were reported so far. Additionally, this FSW variant is found very crucial to enhance the stirring effect of tool due to use of twin tool rotates in opposite direction. In case of CRTT higher frictional heat is generated therefore, low translational and rotational speed is preferable.
Reverse dual rotation FSW (RDR-FSW)	Overheating of weld joint at high speeds leads to the formation of flash defects and undesirable reduction in weld thickness. The reverse dual rotation of pin and shoulder reduces the overheating and enhances material flow. Authors performed welding in a wide range of tool shoulder and pin speeds. In this case improved mechanical properties were observed at a tool rotational speed of N_S: 800rpm, N_P: 800rpm and welding speed of 150-250mm/min. In most of the cases the conical threaded pin profile displays fine grains and improves material flow.
Self-reacting/self-support/ Bobbin tool FSW	Self-reacting or bobbin tool is designed to eliminate the requirement of plunge force and root flaws of conventional friction stir weld joints. Threaded cylindrical pin and scrolled type shoulder improves the flow of material in both the upper and lower parts of the weld joint. In this case higher welding speed and medium tool rotational speed is preferable to attain high quality weld joints.
In situ rolling FSW (IRFSW)	In situ rolling of friction stir weld joints reduces the residual stress and eliminate flash defect. Usually conical threaded pin profile generates sufficient heat input and enhances downward movement of plasticized material. Medium tool rotational speed and welding speed were desirable to enhance properties of the weld joint.

6. Conclusions

The present study discusses various FSW supporting tool systems and their significant role in enhancing weld joints. Table 10 summarizes the effect of process parameters and tool pin profile on weld joint quality. Based on the present investigations, the main findings have been summarized as follows:

1. NRSA-FSW significantly reduces the overheating and extra thinning of weld joint by minimizing flash defects;

2. SR-FSW or bobbin tool eliminates the requirement of plunge force and root flaws of conventional friction stir weld joints. The defects like kissing bonds at the lower end of the weld joint reduce and the vertical application of force is eliminated, making this process energy efficient;

3. Threaded cylindrical pin and scrolled type shoulder of SR-FSW improve the flow of material in both the upper and lower parts of the weld joint. For SR-FSW higher welding speed and medium tool rotational speed is preferable to attain high-quality weld joints;

4. The roller balls of the IRFSW relieve the residual stress of the upper weld surface, reduce the formation of surface imperfections such as flash defects, and enhance the surface appearance;

5. RDR-FSW reduces the overheating of the weld joint and eliminates flash defects and undesirable reduction in weld thickness. The low translational and rotational speed is preferable for NRSA-FSW and CRTT for eliminating flash defects;

6. The overheating effect produced by the CRTT is further minimized by the reverse dual rotation of the tool and shoulder with optimized FSW process parameters, which makes better balance and reduces the chance of overheating, and provides superior quality weld joint.

Authors' contributions

SKL: investigation, methodology, writing-original draft, conceptualization, data curation, writing-reveiw & editing, formal analysis. MB: conceptualization, writing-reveiw & editing, supervision. RB: supervision. SB: formal analysis.

Acknowledgements

References

[1] Thomas WM. Friction stir welding and related friction process characteristics.In: Proceedings of the 7th International Conference Joints in Aluminium - INALCO; 1998; São Carlos, Brazil. Cambridge: Woodhead; 1998. p. 157-174.

[2] Thomas WM, Nicholas ED, Needham JC, Church MG, Templesmith P, Dawes CJ. Imrovements relating to friction stir welding. European Patent Office EP0653265A2, 1994 June 10.

[3] Schneider JA, Nunes AC Jr, Chen PS, Steele G. TEM study of the FSW nugget in AA2195-T81. Journal of Materials Science. 2005;40(16):4341-4345. http://dx.doi.org/10.1007/s10853-005-2808-8.

[4] Silva ACF, De Backer J, Bolmsjö G. Temperature measurements during friction stir welding. International Journal of Advanced Manufacturing Technology. 2017;88(9-12):2899-2908. http://dx.doi.org/10.1007/s00170-016-9007-4.

[5] Behmand SA, Mirsalehi SE, Omidvar H, Safarkhanian MA. Single- and double-pass FSW lap joining of AA5456 sheets with different thicknesses. Materials Science and Technology. 2016;32:438-445. http://dx.doi.org/10.1179/1743284715Y.0000000107.

[6] Hori H, Hino H. Application of friction stir welding to the car body. Weld. Int. 2003;17(4):287-292. http://dx.doi.org/10.1533/wint.2003.3101.

[7] Barnes TA, Pashby IR. Joining techniques for aluminum spaceframes used in automobiles. Part I - solid and liquid phase welding. Journal of Materials Processing Technology. 2000;99:62-71. http://dx.doi.org/10.1016/S0924-0136(99)00367-2.

[8] Thomas WM, Nicholas ED. Friction stir welding for the transportation industries. Materials & Design. 1997;18(4-6):269-273. http://dx.doi.org/10.1016/S0261-3069(97)00062-9.

[9] Wang G, Zhao Y, Hao Y. Friction stir welding of high-strength aerospace aluminum alloy and application in rocket tank manufacturing. Journal of Materials Science and Technology. 2018;34(1):73-91. http://dx.doi.org/10.1016/j.jmst.2017.11.041.

[10] Nandan R, Debroy T, Bhadeshia HKDH. Recent advances in friction-stir welding – Process, weldment structure and properties. Progress in Materials Science. 2008;53(6):980-1023. http://dx.doi.org/10.1016/j.pmatsci.2008.05.001.

[11] Gibson BT, Lammlein DH, Prater TJ, Longhurst WR, Cox CD, Ballun MC, et al. Friction stir welding: process, automation, and control. Journal of Manufacturing Processes. 2014;16(1):56-73. http://dx.doi.org/10.1016/j.jmapro.2013.04.002.

[12]Singh BR. A hand book on friction stir welding. UK: A. Covali; 2016. http://dx.doi.org/10.13140/RG.2.1.5088.6244.

[13] Kumar N, Yuan W, Mishra RS. Friction stir welding of dissimilar alloys and materials. USA: Elsevier, 2015. A framework for friction stir welding of dissimilar alloys and materials, p. 15-33. http://dx.doi.org/10.1016/B978-0-12-802418-8.00002-3.

[14] Threadgilll PL, Leonard AJ, Shercliff HR, Withers PJ. Friction stir welding of aluminium alloys. International Materials Reviews. 2009;54(2):49-93. http://dx.doi.org/10.1179/174328009X411136.

[15] Haldar N, Datta S, Kumar R. Experimental studies on friction-stir welding of AA6061 using Inconel 601 tool. Journal of the Brazilian Society of Mechanical Sciences and Engineering. 2018;40(9):448. http://dx.doi.org/10.1007/s40430-018-1378-z.

[16] Molla Ramezani N, Davoodi B, Aberoumand M, Rezaee Hajideh M. Assessment of tool wear and mechanical properties of Al 7075 nanocomposite in friction stir processing (FSP). Journal of the Brazilian Society of Mechanical Sciences and Engineering. 2019;41(4):1-14. http://dx.doi.org/10.1007/s40430-019-1683-1.

[17] Gan W, Li ZT, Khurana S. Tool materials selection for friction stir welding of L8o steel. Science and Technology of Welding and Joining. 2007;12(7):610-613. http://dx.doi.org/10.1179/174329307X213792.

[18] Hattingh DG, Blignault C, van Niekerk TI, James MN. Characterization of the influences of FSW tool geometry on welding forces and weld tensile strength using an instrumented tool. Journal of Materials Processing Technology. 2008;203(1-3):46-57. http://dx.doi.org/10.1016/j.jmatprotec.2007.10.028.

[19] Elangovan K, Balasubramanian V. Influences of tool pin profile and tool shoulder diameter on the formation of friction stir processing zone in AA6061 aluminium alloy. Materials & Design. 2008;29(2):362-373. http://dx.doi.org/10.1016/j.matdes.2007.01.030.

[20] Kumar B, Widener C, Jahn A, Tweedy B, Cope D, Lee R. Review of the applicability of FSW processing to aircraft applications. In: Proceedings of the 6th AIAA/ASME/ASCE/AHS/ASC Structures, Structural Dynamics and Materials Conference; 2005; Austin, Texas. Austin, Texas: American Institute of Aeronautics and Astronautics; 2005. p. 2483-2500. Collection of Technical Papers - AIAA/ASME/ASCE/AHS/ASC Structures, Structural Dynamics and Materials Conference 4. http://dx.doi.org/10.2514/6.2005-2000.

[21] Haghshenas M, Gerlich AP. Joining of automotive sheet materials by friction-based welding methods: a review. Engineering Science and Technology, an International Journal. 2018;21(1):130-148. http://dx.doi.org/10.1016/j.jestch.2018.02.008.

[22] Uday MB, Fauzi MNA, Zuhailawati H, Ismail AB. Advances in friction welding process: a review. Science and Technology of Welding and Joining. 2010;15(7):534-558. http://dx.doi.org/10.1179/136217110X12785889550064.

[23] Paramaguru D, Pedapati SR, Awang M. A Review on Underwater Friction Stir Welding (UFSW). Singapore: Springer; 2019. http://dx.doi.org/10.1007/978-981-10-9041-7_6.

[24] Patel V, Li W, Vairis A, Badheka V. Recent development in friction stir processing as a solid-state grain refinement technique: microstructural evolution and property enhancement. Critical Reviews in Solid State and Material Sciences. 2019;44(5):378-426. http://dx.doi.org/10.1080/10408436.2018.1490251.

[25] Magalhães VM, Leitão C, Rodrigues DM. Friction stir welding industrialisation and research status. Science and Technology of Welding and Joining. 2018;23(5):400-409. http://dx.doi.org/10.1080/13621718.2017.1403110.

[26] Zhang YN, Cao X, Larose S, Wanjara P. Review of tools for friction stir welding and processing. Canadian Metallurgical Quarterly. 2012;51(3):250-261. http://dx.doi.org/10.1179/1879139512Y.0000000015.

[27] De A, Bhadeshia HKDH, Debroy T. Friction stir welding of mild steel: tool durability and steel microstructure. Materials Science and Technology. 2014;30(9):1050-1056. http://dx.doi.org/10.1179/1743284714Y.0000000534.

[28] Singarapu U, Adepu K, Arumalle SR. Influence of tool material and rotational speed on mechanical properties of friction stir welded AZ31B magnesium alloy. J. Magnes. Alloy. 2015;3(4):335-344. http://dx.doi.org/10.1016/j.jma.2015.10.001.

[29] Shashi Kumar S, Murugan N, Ramachandran KK. Influence of tool material on mechanical and microstructural properties of friction stir welded 316L austenitic stainless steel butt joints. International Journal of Refractory & Hard Metals. 2016;58:196-205. http://dx.doi.org/10.1016/j.ijrmhm.2016.04.015.

[30] Rai R, De A, Bhadeshia HKDH, DebRoy T. Review: friction stir welding tools. Science and Technology of Welding and Joining. 2011;16(4):325-342. http://dx.doi.org/10.1179/1362171811Y.0000000023.

[31] Prado RA, Murr LE, Soto KF, McClure JC. Self-optimization in tool wear for friction-stir welding of Al 6061+20% Al2O3 MMC. Materials Science and Engineering A. 2003;349(1-2):156-165. http://dx.doi.org/10.1016/S0921-5093(02)00750-5.

[32] Çevik B, Özçatalbas Y, Gulenc B. Effect of tool material on micro- Structure and mechanical properties in friction stir welding. Materials Testing. 2016;58(1):36-42. http://dx.doi.org/10.3139/120.110816.

[33] Salari E, Jahazi M, Khodabandeh A, Ghasemi-Nanesa H. Influence of tool geometry and rotational speed on mechanical properties and defect formation in friction stir lap welded 5456 aluminum alloy sheets. Materials & Design. 2014;58:381-389. http://dx.doi.org/10.1016/j.matdes.2014.02.005.

[34] Kumar K, Kailas SV. The role of friction stir welding tool on material flow and weld formation. Materials Science and Engineering A. 2008;485(1-2):367-374. http://dx.doi.org/10.1016/j.msea.2007.08.013.

[35] Ramanjaneyulu K, Madhusudhan Reddy G, Venugopal Rao A, Markandeya R. Structure-property correlation of AA2014 friction stir welds: role of tool pin profile. Journal of Materials Engineering and Performance. 2013;22(8):2224-2240. http://dx.doi.org/10.1007/s11665-013-0512-4.

[36] Quintana KJ, Silveira JLL. Analysis for the forces in FSW for aluminum alloy considering tool geometry and process velocities. Journal of the Brazilian Society of Mechanical Sciences and Engineering. 2018;40(4):229. http://dx.doi.org/10.1007/s40430-018-1162-0.

[37] Scialpi A, De Filippis LAC, Cavaliere P. Influence of shoulder geometry on microstructure and mechanical properties of friction stir welded 6082 aluminium alloy. Materials & Design. 2007;28(4):1124-1129. http://dx.doi.org/10.1016/j.matdes.2006.01.031.

[38] Eslami S, Ramos T, Tavares PJ, Moreira PMGP. Shoulder design developments for FSW lap joints of dissimilar polymers. Journal of Manufacturing Processes. 2015;20:15-23. http://dx.doi.org/10.1016/j.jmapro.2015.09.013.

[39] Wahid MA, Khan ZA, Siddiquee AN. Review on underwater friction stir welding: a variant of friction stir welding with great potential of improving joint properties. Transactions of Nonferrous Metals Society of China. 2018;28(2):193-219. http://dx.doi.org/10.1016/S1003-6326(18)64653-9.

[40] Aissani M, Gachi S, Boubenider F, Benkedda Y. Design and optimization of friction stir welding tool. Materials and Manufacturing Processes. 2010;25(11):1199-1205. http://dx.doi.org/10.1080/10426910903536733.

[41] Trueba L Jr, Heredia G, Rybicki D, Johannes LB. Effect of tool shoulder features on defects and tensile properties of friction stir welded aluminum 6061-T6. Journal of Materials Processing Technology. 2015;219:271-277. http://dx.doi.org/10.1016/j.jmatprotec.2014.12.027.

[42] Arora A, De A, Debroy T. Toward optimum friction stir welding tool shoulder diameter. Scripta Materialia. 2011;64(1):9-12. http://dx.doi.org/10.1016/j.scriptamat.2010.08.052.

[43] Jamshidi Aval H, Serajzadeh S, Kokabi AH, Loureiro A. Effect of tool geometry on mechanical and microstructural behaviours in dissimilar friction stir welding of AA 5086–AA 6061. Science and Technology of Welding and Joining. 2011;16(7):597-604. http://dx.doi.org/10.1179/1362171811Y.0000000044.

[44] Palanivel R, Koshy Mathews P, Murugan N, Dinaharan I. Effect of tool rotational speed and pin profile on microstructure and tensile strength of dissimilar friction stir welded AA5083-H111 and AA6351-T6 aluminum alloys. Materials & Design. 2012;40:7-16. http://dx.doi.org/10.1016/j.matdes.2012.03.027.

[45] Elangovan K, Balasubramanian V. Influences of pin profile and rotational speed of the tool on the formation of friction stir processing zone in AA2219 aluminium alloy. Materials Science and Engineering: A. 2007;459(1-2):7-18. http://dx.doi.org/10.1016/j.msea.2006.12.124.

[46] Elangovan K, Balasubramanian V. Influences of tool pin profile and welding speed on the formation of friction stir processing zone in AA2219 aluminium alloy. Journal of Materials Processing Technology. 2008;200(1-3):163-175. http://dx.doi.org/10.1016/j.jmatprotec.2007.09.019.

[47] Padmanaban G, Balasubramanian V. Selection of FSW tool pin profile, shoulder diameter and material for joining AZ31B magnesium alloy - An experimental approach. Materials & Design. 2009;30(7):2647-2656. http://dx.doi.org/10.1016/j.matdes.2008.10.021.

[48] Ilangovan M, Rajendra Boopathy S, Balasubramanian V. Effect of tool pin profile on microstructure and tensile properties of friction stir welded dissimilar AA 6061–AA 5086 aluminium alloy joints. Def. Technol. 2015;11(2):174-184. http://dx.doi.org/10.1016/j.dt.2015.01.004.

[49] Jamshidi Aval H. Influences of pin profile on the mechanical and microstructural behaviors in dissimilar friction stir welded AA6082-AA7075 butt Joint. Materials & Design. 2015;67:413-421. http://dx.doi.org/10.1016/j.matdes.2014.11.055.

[50] Akinlabi ET. Effect of shoulder size on weld properties of dissimilar metal friction stir welds. Journal of Materials Engineering and Performance. 2012;21(7):1514-1519. http://dx.doi.org/10.1007/s11665-011-0046-6.

[51] Thomas WM, Johnson KI, Wiesner CS. Friction stir welding-recent developments in tool and process technologies. Advanced Engineering Materials. 2003;5(7):485-490. http://dx.doi.org/10.1002/adem.200300355.

[52] Srinivasa Rao MS, Ravi Kumar BVR, Manzoor Hussain M. Experimental study on the effect of welding parameters and tool pin profiles on the IS:65032 aluminum alloy FSW joints. Materials Today: Proceedings. 2017;4(2):1394-1404. http://dx.doi.org/10.1016/j.matpr.2017.01.161.

[53] Azizieh M, Kokabi AH, Abachi P. Effect of rotational speed and probe profile on microstructure and hardness of AZ31/Al2O3 nanocomposites fabricated by friction stir processing. Materials & Design. 2011;32(4):2034-2041. http://dx.doi.org/10.1016/j.matdes.2010.11.055.

[54] Huang G, Cheng D, Wang H, Zhou Q, Shen Y. Effect of tool probe with a disc at the top on the microstructure and mechanical properties of FSW joints for 6061-T6 aluminum alloy. Journal of Adhesion Science and Technology. 2019;33(22):2462-2475. http://dx.doi.org/10.1080/01694243.2019.1645381.

[55] Rao KV. Evaluation of welding characteristics using three-dimensional finite element simulation and experimentation for FSW of aluminum 6061. Journal of the Brazilian Society of Mechanical Sciences and Engineering. 2018;5(2):86. http://dx.doi.org/10.1007/s40430-018-0963-5.

[56] Marzbanrad J, Akbari M, Asadi P, Safaee S. Characterization of the influence of tool pin profile on microstructural and mechanical properties of friction stir welding. Metallurgical and Materials Transactions. B, Process Metallurgy and Materials Processing Science. 2014;45(5):1887-1894. http://dx.doi.org/10.1007/s11663-014-0089-9.

[57] Bayazid SM, Farhangi H, Ghahramani A. Effect of pin profile on defects of friction stir welded 7075 aluminum alloy. Procedia Materials Science. 2015;11:12-16. http://dx.doi.org/10.1016/j.mspro.2015.11.013.

[58] Rajakumar S, Balasubramanian V. Establishing relationships between mechanical properties of aluminium alloys and optimised friction stir welding process parameters. Materials & Design. 2012;40:17-35. http://dx.doi.org/10.1016/j.matdes.2012.02.054.

[59] Kimapong K, Watanabe T. Effect of welding process parameters on mechanical property of FSW lap joint between aluminum alloy and steel. Materials Transactions. 2005;46(10):2211-2217. http://dx.doi.org/10.2320/matertrans.46.2211.

[60] Babu S, Elangovan K, Balasubramanian V, Balasubramanian M. Optimizing friction stir welding parameters to maximize tensile strength of AA2219 aluminum alloy joints. Metals and Materials International. 2009;15(2):321-330. http://dx.doi.org/10.1007/s12540-009-0321-3.

[61] do Vale NL, Torres EA, Santos TFA, Urtiga SL Fo, dos Santos JF. Effect of the energy input on the microstructure and mechanical behavior of AA2024-T351 joint produced by friction stir welding. Journal of the Brazilian Society of Mechanical Sciences and Engineering. 2018;40(9):467. http://dx.doi.org/10.1007/s40430-018-1372-5.

[62] Shojaeefard MH, Khalkhali A, Akbari M, Tahani M. Application of Taguchi optimization technique in determining aluminum to brass friction stir welding parameters. Materials & Design. 2013;52:587-592. http://dx.doi.org/10.1016/j.matdes.2013.06.003.

[63] Esmaeili A, Zareie Rajani HR, Sharbati M, Givi MKB, Shamanian M. The role of rotation speed on intermetallic compounds formation and mechanical behavior of friction stir welded brass/aluminum 1050 couple. Intermetallics. 2011;19(11):1711-1719. http://dx.doi.org/10.1016/j.intermet.2011.07.006.

[64] Galvão I, Oliveira JC, Loureiro A, Rodrigues DM. Formation and distribution of brittle structures in friction stir welding of aluminium and copper: influence of process parameters. Science and Technology of Welding and Joining. 2011;16(8):681-689. http://dx.doi.org/10.1179/1362171811Y.0000000057.

[65] Cao F, Li J, Hou W, Shen Y, Ni R. Microstructural evolution and mechanical properties of the friction stir welded Al–Cu dissimilar joint enhanced by post-weld heat treatment. Materials Characterization. 2021;174:110998. http://dx.doi.org/10.1016/j.matchar.2021.110998.

[66] Felix Xavier Muthu M, Jayabalan V. Effect of pin profile and process parameters on microstructure and mechanical properties of friction stir welded Al-Cu joints. Transactions of Nonferrous Metals Society of China. 2016;26(4):984-993. http://dx.doi.org/10.1016/S1003-6326(16)64195-X.

[67] Abdollah-Zadeh A, Saeid T, Sazgari B. Microstructural and mechanical properties of friction stir welded aluminum/copper lap joints. Journal of Alloys and Compounds. 2008;460(1-2):535-538. http://dx.doi.org/10.1016/j.jallcom.2007.06.009.

[68] Bisadi H, Tavakoli A, Tour Sangsaraki M, Tour Sangsaraki K. The influences of rotational and welding speeds on microstructures and mechanical properties of friction stir welded Al5083 and commercially pure copper sheets lap joints. Materials & Design. 2013;43:80-88. http://dx.doi.org/10.1016/j.matdes.2012.06.029.

[69] Moshwan R, Yusof F, Hassan MA, Rahmat SM. Effect of tool rotational speed on force generation, microstructure and mechanical properties of friction stir welded Al-Mg-Cr-Mn (AA 5052-O) alloy. Materials & Design. 2015;66:118-128. http://dx.doi.org/10.1016/j.matdes.2014.10.043.

[70] Singh S, Singh G, Prakash C, Kumar R. On the mechanical characteristics of friction stir welded dissimilar polymers: statistical analysis of the processing parameters and morphological investigations of the weld joint. Journal of the Brazilian Society of Mechanical Sciences and Engineering. 2020;42(4):154. http://dx.doi.org/10.1007/s40430-020-2227-4.

[71] Akinlabi ET, Els-Botes A, McGrath PJ. Effect of travel speed on joint properties of dissimilar metal friction stir welds. In: Proceedings of 2nd International Conference on Advances in Engineering and Technology (AET). USA: AET; 2011. p. 155-161.

[72] Fotouhi Y, Rasaee S, Askari A, Bisadi H. Properties in dissimilar butt friction stir welding of al5083–copper sheets. Eng. Solid Mech. 2014;2(3):239-246. http://dx.doi.org/10.5267/j.esm.2014.3.001.

[73] Muthu MFX, Jayabalan V. Tool travel speed effects on the microstructure of friction stir welded aluminum-copper joints. Journal of Materials Processing Technology. 2015;217:105-113. http://dx.doi.org/10.1016/j.jmatprotec.2014.11.007.

[74] Rajakumar S, Muralidharan C, Balasubramanian V. Influence of friction stir welding process and tool parameters on strength properties of AA7075-T6 aluminium alloy joints. Materials & Design. 2011;32(2):535-549. http://dx.doi.org/10.1016/j.matdes.2010.08.025.

[75] Mehta KP, Badheka VJ. Influence of tool design and process parameters on dissimilar friction stir welding of copper to AA6061-T651 joints. International Journal of Advanced Manufacturing Technology. 2015;80(9-12):2073-2082. http://dx.doi.org/10.1007/s00170-015-7176-1.

[76]   Kumar R, Singh K, Pandey S. Process forces and heat input as function of process parameters in AA5083 friction stir welds. Transactions of Nonferrous Metals Society of China. 2012;22(2):288-298. http://dx.doi.org/10.1016/S1003-6326(11)61173-4.

[77] Chien CH, Lin WB, Chen T. Optimal FSW process parameters for aluminum alloys AA5083. Zhongguo Gongcheng Xuekan. 2011;34(1):99-105. http://dx.doi.org/10.1080/02533839.2011.553024.

[78] Kumar S, Acharya U, Sethi D, Medhi T, Roy BS, Saha SC. Effect of traverse speed on microstructure and mechanical properties of friction-stir-welded third-generation Al–Li alloy. Journal of the Brazilian Society of Mechanical Sciences and Engineering. 2020;42(8):423. http://dx.doi.org/10.1007/s40430-020-02509-w.

[79] Lombard H, Hattingh DG, Steuwer A, James MN. Optimising FSW process parameters to minimise defects and maximise fatigue life in 5083-H321 aluminium alloy. Engineering Fracture Mechanics. 2008;75(3-4):341-354. http://dx.doi.org/10.1016/j.engfracmech.2007.01.026.

[80] Abolusoro OP, Akinlabi ET, Kailas SV. Tool rotational speed impact on temperature variations, mechanical properties and microstructure of friction stir welding of dissimilar high-strength aluminium alloys. Journal of the Brazilian Society of Mechanical Sciences and Engineering. 2020;42(4):176. http://dx.doi.org/10.1007/s40430-020-2259-9.

[81] Lertora E, Gambaro C. AA8090 Al-Li Alloy FSW parameters to minimize defects and increase fatigue life. International Journal of Material Forming. 2010;3(S1):1003-1006. http://dx.doi.org/10.1007/s12289-010-0939-1.

[82] Lombard H, Hattingh DG, Steuwer A, James MN. Effect of process parameters on the residual stresses in AA5083-H321 friction stir welds. Materials Science and Engineering A. 2009;501(1-2):119-124. http://dx.doi.org/10.1016/j.msea.2008.09.078.

[83] Lader SK, Baruah M, Ballav R. Improvement in the weldability and mechanical properties of CuZn40 and AA1100-O dissimilar joints by underwater friction stir welding. Journal of Manufacturing Processes. 2023;85:1154-1172. http://dx.doi.org/10.1016/j.jmapro.2022.12.033.

[84] Lader SK, Baruah M, Ballav R. Significance of underwater friction stir welding on the weld integrity of thin sheets of aluminum (AA1050-O) and brass (CuZn34) joints. Materials Science and Engineering A. 2023;865:144627. http://dx.doi.org/10.1016/j.msea.2023.144627.

[85] Mahto RP, Gupta C, Kinjawadekar M, Meena A, Pal SK. Weldability of AA6061-T6 and AISI 304 by underwater friction stir welding. Journal of Manufacturing Processes. 2019;38:370-386. http://dx.doi.org/10.1016/j.jmapro.2019.01.028.

[86] Shultz EF, Cole EG, Smith CB, Zinn MR, Ferrier NJ, Pfefferkorn FE. Effect of compliance and travel angle on friction stir welding with gaps. Journal of Manufacturing Science and Engineering. 2010;132(4):0410101-0410109. http://dx.doi.org/10.1115/1.4001581.

[87] Nakata K, Kim YG, Ushio M, Hashimoto T, Jyogan S. Weldability of high strength aluminum alloys by friction stir welding. ISIJ International. 2000;40(Suppl):S15-S19. http://dx.doi.org/10.2355/isijinternational.40.Suppl_S15.

[88] Mehta KP, Badheka VJ. Experimental Investigation of Process Parameters on Defects Generation in Copper to AA6061-T651 friction stir Welding, Int. J. Adv. Mech. Automob. Eng. 2016;3(1). http://dx.doi.org/10.15242/IJAMAE.E0316007.

[89] Leal R, Loureiro A. Defects formation in friction stir welding of aluminium alloys. Materials Science Forum. 2004;455-456:299-302. http://dx.doi.org/10.4028/www.scientific.net/MSF.455-456.299.

[90] Podržaj P, Jerman B, Klobčar D. Welding defects at friction stir welding. Metalurgija. 2015;54(2):387-389.

[91] Le Jolu T, Morgeneyer TF, Denquin A, Sennour M, Laurent A, Besson J, et al. Microstructural characterization of internal welding defects and their effect on the tensile behavior of FSW Joints of AA2198 Al-Cu-Li alloy. Metallurgical and Materials Transactions. A, Physical Metallurgy and Materials Science. 2014;45(12):5531-5544. http://dx.doi.org/10.1007/s11661-014-2537-1.

[92] Padhy GK, Wu CS, Gao S. Auxiliary energy assisted friction stir welding – Status review. Science and Technology of Welding and Joining. 2015;20(8):631-649. http://dx.doi.org/10.1179/1362171815Y.0000000048.

[93] Tang J, Shen Y. Effects of preheating treatment on temperature distribution and material flow of aluminum alloy and steel friction stir welds. Journal of Manufacturing Processes. 2017;29:29-40. http://dx.doi.org/10.1016/j.jmapro.2017.07.005.

[94] Verma S, Gupta M, Misra JP. Effect of preheating and water cooling on the performance of friction-stir-welded aviation-grade aluminum alloy joints. Journal of Materials Engineering and Performance. 2019;28(7):4209-4220. http://dx.doi.org/10.1007/s11665-019-04183-z.

[95] Safi SV, Amirabadi H, Besharati Givi MK, Safi SM. The effect of preheating on mechanical properties of friction stir welded dissimilar joints of pure copper and AA7075 aluminum alloy sheets. International Journal of Advanced Manufacturing Technology. 2016;84(9-12):2401-2411. http://dx.doi.org/10.1007/s00170-015-7877-5.

[96] Elanchezhian C, Vijaya Ramnath B, Pazhanivel K, Vedhapuri A, Mano B, Manojkumar A, et al. Comparative Study and Analysis of Friction Stir Welding with Plasma ARC Welding. Applied Mechanics and Materials. 2015;766–767:695-700. http://dx.doi.org/10.4028/www.scientific.net/AMM.766-767.695.

[97] Fei X, Jin X, Ye Y, Xiu T, Yang H. Effect of pre-hole offset on the property of the joint during laser-assisted friction stir welding of dissimilar metals steel and aluminum alloys. Materials Science and Engineering A. 2016;653:43-52. http://dx.doi.org/10.1016/j.msea.2015.11.101.

[98] Bang HS, Bang HS, Jeon GH, Oh IH, Ro CS. Gas tungsten arc welding assisted hybrid friction stir welding of dissimilar materials Al6061-T6 aluminum alloy and STS304 stainless steel. Materials & Design. 2012;37:48-55. http://dx.doi.org/10.1016/j.matdes.2011.12.018.

[99] Zhang Z, Zhang HW. Numerical studies of preheating time effect on temperature and material behaviours in friction stir welding process. Science and Technology of Welding and Joining. 2007;12(5):436-448. http://dx.doi.org/10.1179/174329307X214386.

[100] Aydin M. Effects of welding parameters and pre-heating on the friction stir welding of UHMW-polyethylene. Polymer-Plastics Technology and Engineering. 2010;49(6):595-601. http://dx.doi.org/10.1080/03602551003664503.

[101] Suleimanov RI, Zainagalina LZ, Khabibullin MY, Zaripova LM, Kovalev NO. Studying heat-affected zone deformations of electric arc welding. IOP Conference Series: Materials Science and Engineering. 2018;327:032053. http://dx.doi.org/10.1088/1757-899X/327/3/032053.

[102] Li B, Shen Y. The investigation of abnormal particle-coarsening phenomena in friction stir repair weld of 2219-T6 aluminum alloy. Materials & Design. 2011;32(7):3796-3802. http://dx.doi.org/10.1016/j.matdes.2011.03.029.

[103] Starink MJ, Deschamps A, Wang SC. The strength of friction stir welded and friction stir processed aluminium alloys. Scripta Materialia. 2008;58(5):377-382. http://dx.doi.org/10.1016/j.scriptamat.2007.09.061.

[104] Li WY, Fu T, Hütsch L, Hilgert J, Wang FF, dos Santos JF, et al. Effects of tool rotational and welding speed on microstructure and mechanical properties of bobbin-tool friction-stir welded Mg AZ31. Materials & Design. 2014;64:714-720. http://dx.doi.org/10.1016/j.matdes.2014.07.023.

[105] Huang Y, Wan L, Lv S, Zhang J, Fu G. In situ rolling friction stir welding for joining AA2219. Materials & Design. 2013;50:810-816. http://dx.doi.org/10.1016/j.matdes.2013.03.088.

[106] Shi L, Wu CS, Liu HJ. The effect of the welding parameters and tool size on the thermal process and tool torque in reverse dual-rotation friction stir welding. International Journal of Machine Tools & Manufacture. 2015;91:1-11. http://dx.doi.org/10.1016/j.ijmachtools.2015.01.004.

[107] Russell MJ, Threadgill PL, Thomas MJ, Wynne BP. Static shoulder friction stir welding of Ti–6Al–4V; process and evaluation. In: Proceedings of the 11th World Conference on titanium (Ti-2007), (JIMIC - 5); 2007 June 3-7; Kyoto, Japan. United Kingdom: TWI; 2007. p. 1095-1098.

[108] Russell MJ, Blignault C, Horrex NL, Wiesner CS. Recent developments in the friction stir welding of titanium alloys. Welding in the World. 2008;52(9-10):12-15. http://dx.doi.org/10.1007/BF03266662.

[109] Sejani D, Li W, Patel V. Stationary shoulder friction stir welding–low heat input joining technique: a review in comparison with conventional FSW and bobbin tool FSW. Critical Reviews in Solid State and Material Sciences. 2022;47(6):865-914. http://dx.doi.org/10.1080/10408436.2021.1935724.

[110] You J, Zhao Y, Dong C, Wang C, Miao S, Yi Y, et al. Microstructure characteristics and mechanical properties of stationary shoulder friction stir welded 2219-T6 aluminium alloy at high rotation speeds. International Journal of Advanced Manufacturing Technology. 2020;108(4):987-996. http://dx.doi.org/10.1007/s00170-019-04594-1.

[111] Ji SD, Meng XC, Liu JG, Zhang LG, Gao SS. Formation and mechanical properties of stationary shoulder friction stir welded 6005A-T6 aluminum alloy. Materials & Design. 2014;62:113-117. http://dx.doi.org/10.1016/j.matdes.2014.05.016.

[112] Avettand-Fènoël MN, Taillard R. Effect of a pre or postweld heat treatment on microstructure and mechanical properties of an AA2050 weld obtained by SSFSW. Materials & Design. 2016;89:348-361. http://dx.doi.org/10.1016/j.matdes.2015.09.151.

[113] Li D, Yang X, Cui L, He F, Shen H. Effect of welding parameters on microstructure and mechanical properties of AA6061-T6 butt welded joints by stationary shoulder friction stir welding. Materials & Design. 2014;64:251-260. http://dx.doi.org/10.1016/j.matdes.2014.07.046.

[114] Chen Y, Li H, Wang X, Ding H, Zhang F. A comparative investigation on conventional and stationary shoulder friction stir welding of Al-7075 butt-lap structure. Metals. 2019;9(12):1264. http://dx.doi.org/10.3390/met9121264.

[115] Yue Y, Zhou Z, Ji S, Zhang J, Li Z. Effect of welding speed on joint feature and mechanical properties of friction stir lap welding assisted by external stationary shoulders. International Journal of Advanced Manufacturing Technology. 2017;89(5-8):1691-1698. http://dx.doi.org/10.1007/s00170-016-9240-x.

[116] Ji S, Li Z, Zhou Z, Zhang L. Microstructure and mechanical property differences between friction stir lap welded joints using rotating and stationary shoulders. International Journal of Advanced Manufacturing Technology. 2017;90(9-12):3045-3053. http://dx.doi.org/10.1007/s00170-016-9640-y.

[117] Huang Y, Meng X, Xie Y, Li J, Si X, Fan Q. Improving mechanical properties of composite/metal friction stir lap welding joints via a taper-screwed pin with triple facets. Journal of Materials Processing Technology. 2019;268:80-86. http://dx.doi.org/10.1016/j.jmatprotec.2019.01.011.

[118] Xu Z, Li Z, Lv Z, Zhang L. Effect of welding speed on joint features and lap shear properties of stationary shoulder FSLWed Alclad 2024 al alloy. Journal of Materials Engineering and Performance. 2017;26(3):1358-1364. http://dx.doi.org/10.1007/s11665-017-2527-8.

[119] Barbini A, Carstensen J, dos Santos JF. Influence of a non-rotating shoulder on heat generation, microstructure and mechanical properties of dissimilar AA2024/AA7050 FSW joints. Journal of Materials Science and Technology. 2018;34(1):119-127. http://dx.doi.org/10.1016/j.jmst.2017.10.017.

[120] Wu B, Liu J, Song Q, Lv Z, Bai W. Controllability of joint integrity and mechanical properties of friction stir welded 6061-T6 aluminum and AZ31B magnesium alloys based on stationary shoulder. High-Temperature Materials and Processes. 2019;38(2019):557-566. http://dx.doi.org/10.1515/htmp-2019-0001.

[121] Li JQ, Liu HJ. Design of tool system for the external nonrotational shoulder assisted friction stir welding and its experimental validations on 2219-T6 aluminum alloy. International Journal of Advanced Manufacturing Technology. 2013;66(5-8):623-634. http://dx.doi.org/10.1007/s00170-012-4353-3.

[122] Li Z, Yue Y, Ji S, Chai P, Zhou Z. Joint features and mechanical properties of friction stir lap welded alclad 2024 aluminum alloy assisted by external stationary shoulder. Materials & Design. 2016;90:238-247. http://dx.doi.org/10.1016/j.matdes.2015.10.056.

[123] Buffa G, Fratini L, Impero F, Masnata A, Scherillo F, Squillace A. Surface and mechanical characterization of stationary shoulder friction stir welded lap joints: experimental and numerical approach. International Journal of Material Forming. 2020;13(5):725-736. http://dx.doi.org/10.1007/s12289-020-01574-9.

[124] Ding RJ, Oelgoetz PA. Auto-adjustable pin tool for friction stir welding. United States patent 5893507. 1999 Apr 13.

[125] Kumari K, Pal SK, Singh SB. S. BratSingh, Friction stir welding by using counter-rotating twin tool. Journal of Materials Processing Technology. 2015;215:132-141. http://dx.doi.org/10.1016/j.jmatprotec.2014.07.031.

[126] Jain R, Kumari K, Pal SK, Singh SB. Counter rotating twin-tool system in friction stir welding process: A simulation study. Journal of Materials Processing Technology. 2018;255:121-128. http://dx.doi.org/10.1016/j.jmatprotec.2017.11.043.

[127] Starink MJ, Deschamps A, Wang SC. The strength of friction stir welded and friction stir processed aluminium alloys. Scripta Materialia. 2008;58(5):377-382. http://dx.doi.org/10.1016/j.scriptamat.2007.09.061.

[128] Li B, Shen Y. The investigation of abnormal particle-coarsening phenomena in friction stir repair weld of 2219-T6 aluminum alloy. Materials & Design. 2011;32(7):3796-3802. http://dx.doi.org/10.1016/j.matdes.2011.03.029.

[129] Kim YG, Fujii H, Tsumura T, Komazaki T, Nakata K. Three defect types in friction stir welding of aluminum die casting alloy. Materials Science and Engineering A. 2006;415(1-2):250-254. http://dx.doi.org/10.1016/j.msea.2005.09.072.

[130] Liu H, Nakata K, Yamamoto N, Liao J. Friction stir welding of pure titanium lap joint. Science and Technology of Welding and Joining. 2010;15(5):428-432. http://dx.doi.org/10.1179/136217110X12731414740031.

[131] Li JQ, Liu HJ. Characteristics of the reverse dual-rotation friction stir welding conducted on 2219-T6 aluminum alloy. Materials & Design. 2013;45:148-154. http://dx.doi.org/10.1016/j.matdes.2012.08.068.

[132] Liu HJ, Li JQ, Duan WJ. Research on reverse dual rotation friction stir welding process. Proceedings of the 1st International Joint Symposium on Joining and Weldin. 2013:25-32. http://dx.doi.org/10.1533/978-1-78242-164-1.25.

[133] Thomas WM, Kallee SW, Staines DG, Oakley PJ. Friction stir welding - Process variants and developments in the automotive industry. In: Proceedings of the SAE 2006 World Congress & Exhibition; 2006; USA. USA: SAE International; 2006. p. 1-8. SAE Technical Paper. http://dx.doi.org/10.4271/2006-01-0555.

[134] Li JQ, Liu HJ. Effects of welding speed on microstructures and mechanical properties of AA2219-T6 welded by the reverse dual-rotation friction stir welding. International Journal of Advanced Manufacturing Technology. 2013;68(9-12):2071-2083. http://dx.doi.org/10.1007/s00170-013-4812-5.

[135] Li JQ, Liu HJ. Effects of the reversely rotating assisted shoulder on microstructures during the reverse dual-rotation friction stir welding. Journal of Materials Science and Technology. 2015;31(4):375-383. http://dx.doi.org/10.1016/j.jmst.2014.07.020.

[136] Li JQ, Liu HJ. Effects of tool rotation speed on microstructures and mechanical properties of AA2219-T6 welded by the external non-rotational shoulder assisted friction stir welding. Materials & Design. 2013;43:299-306. http://dx.doi.org/10.1016/j.matdes.2012.07.011.

[137] Mohammadi J, Behnamian Y, Mostafaei A, Izadi H, Saeid T, Kokabi AH, et al. Friction stir welding joint of dissimilar materials between AZ31B magnesium and 6061 aluminum alloys: microstructure studies and mechanical characterizations. Materials Characterization. 2015;101:189-207. http://dx.doi.org/10.1016/j.matchar.2015.01.008.

[138] Li JQ, Liu HJ. Optimization of welding parameters for the reverse dual-rotation friction stir welding of a high-strength aluminum alloy 2219-T6. International Journal of Advanced Manufacturing Technology. 2014;76(5-8):1469-1478. http://dx.doi.org/10.1007/s00170-014-6352-z.

[139] Jamshidi Aval H, Loureiro A. Effect of reverse dual rotation process on properties of friction stir welding of AA7075 to AISI304. Transactions of Nonferrous Metals Society of China. 2019;29(5):964-975. http://dx.doi.org/10.1016/S1003-6326(19)65005-3.

[140] Shi L, Wu CS, Liu HJ. Analysis of heat transfer and material flow in reverse dual-rotation friction stir welding. Welding in the World. 2015;59(5):629-638. http://dx.doi.org/10.1007/s40194-015-0238-z.

[141] Shi L, Wu CS, Liu HJ. Modeling the material flow and heat transfer in reverse dual-rotation friction stir welding. Journal of Materials Engineering and Performance. 2014;23(8):2918-2929. http://dx.doi.org/10.1007/s11665-014-1042-4.

[142] Singh RKR, Sharma C, Dwivedi DK, Mehta NK, Kumar P. The microstructure and mechanical properties of friction stir welded Al-Zn-Mg alloy in as welded and heat treated conditions. Materials & Design. 2011;32(2):682-687. http://dx.doi.org/10.1016/j.matdes.2010.08.001.

[143] Bansal A, Singla AK, Dwivedi V, Goyal DK, Singla J, Gupta MK, et al. Influence of cryogenic treatment on mechanical performance of friction stir Al-Zn-Cu alloy weldments. Journal of Manufacturing Processes. 2020;56:43-53. http://dx.doi.org/10.1016/j.jmapro.2020.04.067.

[144] Mehdi H, Mishra RS. Analysis of material flow and heat transfer in reverse dual rotation friction stir welding: a review. International Journal of Steel Structures. 2019;19(2):422-434. http://dx.doi.org/10.1007/s13296-018-0131-x.

[145] Zhou L, Zhang RX, Hu XY, Guo N, Zhao HH, Huang YX. Effects of rotation speed of assisted shoulder on microstructure and mechanical properties of 6061-T6 aluminum alloy by dual-rotation friction stir welding. International Journal of Advanced Manufacturing Technology. 2019;100(1-4):199-208. http://dx.doi.org/10.1007/s00170-018-2570-0.

[146] Zhou L, Zhang RX, Hu XY, Guo N, Zhao HH, Huang YX. Effects of rotation speed of assisted shoulder on microstructure and mechanical properties of 6061-T6 aluminum alloy by dual-rotation friction stir welding. International Journal of Advanced Manufacturing Technology. 2019;100(1-4):199-208. http://dx.doi.org/10.1007/s00170-018-2570-0.

[147] Li JQ, Liu HJ. Optimization of welding parameters for the reverse dual-rotation friction stir welding of a high-strength aluminum alloy 2219-T6. International Journal of Advanced Manufacturing Technology. 2014;76(5-8):1469-1478. http://dx.doi.org/10.1007/s00170-014-6352-z.

[148] Zhao S, Bi Q, Wang Y, Shi J. Empirical modeling for the effects of welding factors on tensile properties of bobbin tool friction stir-welded 2219-T87 aluminum alloy. International Journal of Advanced Manufacturing Technology. 2017;90(1-4):1105-1118. http://dx.doi.org/10.1007/s00170-016-9450-2.

[149] Malarvizhi S, Balasubramanian V. Influences of tool shoulder diameter to plate thickness ratio (D/T) on stir zone formation and tensile properties of friction stir welded dissimilar joints of AA6061 aluminum-AZ31B magnesium alloys. Materials & Design. 2012;40:453-460. http://dx.doi.org/10.1016/j.matdes.2012.04.008.

[150] Azizieh M, Sadeghi Alavijeh A, Abbasi M, Balak Z, Kim HS. Mechanical properties and microstructural evaluation of AA1100 to AZ31 dissimilar friction stir welds. Materials Chemistry and Physics. 2016;170:251-260. http://dx.doi.org/10.1016/j.matchemphys.2015.12.046.

[151] Sato YS, Park SHC, Michiuchi M, Kokawa H. Constitutional liquation during dissimilar friction stir welding of Al and Mg alloys. Scripta Materialia. 2004;50(9):1233-1236. http://dx.doi.org/10.1016/j.scriptamat.2004.02.002.

[152] Wang FF, Li WY, Shen J, Hu SY, dos Santos JF. Effect of tool rotational speed on the microstructure and mechanical properties of bobbin tool friction stir welding of Al-Li alloy. Materials & Design. 2015;86:933-940. http://dx.doi.org/10.1016/j.matdes.2015.07.096.

[153] Zhou L, Li GH, Liu CL, Wang J, Huang YX, Feng JC, et al. Microstructural characteristics and mechanical properties of Al–Mg–Si alloy self-reacting friction stir welded joints. Science and Technology of Welding and Joining. 2017;22(5):438-445. http://dx.doi.org/10.1080/13621718.2016.1251733.

[154] Sued MK, Pons D, Lavroff J, Wong EH. Design features for bobbin friction stir welding tools: development of a conceptual model linking the underlying physics to the production process. Materials & Design. 2014;54:632-643. http://dx.doi.org/10.1016/j.matdes.2013.08.057.

[155] Liu HJ, Hou JC, Guo H. Effect of welding speed on microstructure and mechanical properties of self-reacting friction stir welded 6061-T6 aluminum alloy. Materials & Design. 2013;50:872-878. http://dx.doi.org/10.1016/j.matdes.2013.03.105.

[156] Tabatabaeipour M, Hettler J, Delrue S, Van Den Abeele K. NDT & E International Non-destructive ultrasonic examination of root defects in friction stir welded butt-joints. NDT & E International. 2016;80:23-34. http://dx.doi.org/10.1016/j.ndteint.2016.02.007.

[157] Xu W, Wang H, Luo Y, Li W, Fu MW. Mechanical behavior of 7085-T7452 aluminum alloy thick plate joint produced by double-sided friction stir welding: effect of welding parameters and strain rates. Journal of Manufacturing Processes. 2018;35:261-270. http://dx.doi.org/10.1016/j.jmapro.2018.07.028.

[158] Zhou C, Yang X, Luan G. Effect of kissing bond on fatigue behavior of friction stir welds on Al 5083 alloy. Journal of Materials Science. 2006;41(10):2771-2777. http://dx.doi.org/10.1007/s10853-006-6337-x.

[159] Zhou C, Yang X, Luan G. Effect of root flaws on the fatigue property of friction stir welds in 2024-T3 aluminum alloys. Materials Science and Engineering: A. 2006;418(1-2):155-160. http://dx.doi.org/10.1016/j.msea.2005.11.042.

[160] Simoncini M, Cabibbo M, Forcellese A. Development of double-side friction stir welding to improve post-welding formability of joints in AA6082 aluminium alloy. Proceedings of the Institution of Mechanical Engineers, Part B: Journal of Engineering Manufacture. 2016;230(5):807-817. http://dx.doi.org/10.1177/0954405414560618.

[161] Hejazi I, Mirsalehi SE. Effect of pin penetration depth on double-sided friction stir welded joints of AA6061-T913 alloy. Transactions of Nonferrous Metals Society of China. 2016;26(3):676-683. http://dx.doi.org/10.1016/S1003-6326(16)64158-4.

[162] Barnes SJ, Steuwer A, Mahawish S, Johnson R, Withers PJ. Residual strains and microstructure development in single and sequential double sided friction stir welds in RQT-701 steel. Materials Science and Engineering A. 2008;492(1-2):35-44. http://dx.doi.org/10.1016/j.msea.2008.02.049.

[163] Mehra S, Dhanda P, Khanna R , Goyat NS, Verma S. Effect of tool on tensile strength in single and double sided friction stir welding. International Journal of Scientific & Engineering Research. 2012;3(11):1-6.

[164] Chen J, Fujii H, Sun Y, Morisada Y, Kondoh K. Optimization of mechanical properties of fine-grained non-combustive magnesium alloy joint by asymmetrical double-sided friction stir welding. Journal of Materials Processing Technology. 2017;242:117-125. http://dx.doi.org/10.1016/j.jmatprotec.2016.11.021.

[165] Zhang H, Wang M, Zhang X, Yang G. Microstructural characteristics and mechanical properties of bobbin tool friction stir welded 2A14-T6 aluminum alloy. Materials & Design. 2015;65:559-566. http://dx.doi.org/10.1016/j.matdes.2014.09.068.

[166] Esmaily M, Mortazavi N, Osikowicz W, Hindsefelt H, Svensson JE, Halvarsson M, et al. Bobbin and conventional friction stir welding of thick extruded AA6005-T6 profiles. Materials & Design. 2016;108:114-125. http://dx.doi.org/10.1016/j.matdes.2016.06.089.

[167] Liu HJ, Hou JC, Guo H. Effect of welding speed on microstructure and mechanical properties of self-reacting friction stir welded 6061-T6 aluminum alloy. Materials & Design. 2013;50:872-878. http://dx.doi.org/10.1016/j.matdes.2013.03.105.

[168] Sued MK, Pons D, Lavroff J, Wong EH. Design features for bobbin friction stir welding tools: development of a conceptual model linking the underlying physics to the production process. Materials & Design. 2014;54:632-643. http://dx.doi.org/10.1016/j.matdes.2013.08.057.

[169] Huang YX, Wan L, Lv SX, Feng JC. Novel design of tool for joining hollow extrusion by friction stir welding. Science and Technology of Welding and Joining. 2013;18(3):239-246. http://dx.doi.org/10.1179/1362171812Y.0000000096.

[170] Hou JC, Liu HJ, Zhao YQ. Influences of rotation speed on microstructures and mechanical properties of 6061-T6 aluminum alloy joints fabricated by self-reacting friction stir welding tool. International Journal of Advanced Manufacturing Technology. 2014;73(5-8):1073-1079. http://dx.doi.org/10.1007/s00170-014-5857-9.

[171] Okamoto K, Sato A, Park SH, Hirano S. Microstructure and Mechanical Properties of FSWed Aluminum Extrusion with Bobbin Tools. Materials Science Forum. 2012;709:990-995. http://dx.doi.org/10.4028/www.scientific.net/MSF.706-709.990.

[172] Wan L, Huang Y, Guo W, Lv S, Feng J. Mechanical Properties and Microstructure of 6082-T6 Aluminum Alloy Joints by Self-support Friction Stir Welding. Journal of Materials Science and Technology. 2014;30(12):1243-1250. http://dx.doi.org/10.1016/j.jmst.2014.04.009.

[173] Wang FF, Li WY, Shen J, Wen Q. Improving weld formability by a novel dual-rotation bobbin toolfriction stir welding. Journal of Materials Science and Technology. 2017;1–5. http://dx.doi.org/10.1016/j.jmst.2017.11.001.

[174] Wan L, Huang Y, Lv Z, Lv S, Feng J. Effect of self-support friction stir welding on microstructure and microhardness of 6082-T6 aluminum alloy joint. Materials & Design. 2014;55:197-203. http://dx.doi.org/10.1016/j.matdes.2013.09.073.

[175] Zhao Y, Wang C, Dong C. Microstructural characteristics and mechanical properties of water cooling bobbin-tool friction stir welded 6063-T6 aluminum alloy. MATEC Web of Conferences. 2018;03002. https://doi.org/10.1051/matecconf/201820603002.

[176] Yang C, Ni DR, Xue P, Xiao BL, Wang W, Wang KS, et al. Materials characterization a comparative research on bobbin tool and conventional friction stir welding of Al-Mg-Si alloy plates. Materials Characterization. 2018;145:20-28. http://dx.doi.org/10.1016/j.matchar.2018.08.027.

[177] Li GH, Zhou L, Luo SF, Du ZY, Feng JC, Meng FX. Microstructure and mechanical properties of self-reacting friction stir welded AA2219-T87 aluminium alloy. Science and Technology of Welding and Joining. 2020;25(2):142-149. http://dx.doi.org/10.1080/13621718.2019.1648719.

[178] Goebel J, Reimann M, Norman A, dos Santos JF. Semi-stationary shoulder bobbin tool friction stir welding of AA2198-T851. Journal of Materials Processing Technology. 2017;245:37-45. http://dx.doi.org/10.1016/j.jmatprotec.2017.02.011.

[179] Thomas WM, Wiesner CS. Recent developments of FSW technologies: evaluation of root defects, composite refractory tools for steel joining and one-pass welding of thick sections using self-reacting bobbin tools. ASM Proceedings of the International Conference Trends in Welding Research. 2009:25-34. https://doi.org/10.1361/cp2008twr025.

[180] Kadlec M, Růžek R, Nováková L. Mechanical behaviour of AA 7475 friction stir welds with the kissing bond defect. International Journal of Fatigue. 2015;74:7-19. http://dx.doi.org/10.1016/j.ijfatigue.2014.12.011.

[181] Thomas WM, Wiesner CS, Marks DJ, Staines DG. Conventional and bobbin friction stir welding of 12% chromium alloy steel using composite refractory tool materials. Science and Technology of Welding and Joining. 2009;14(3):247-253. http://dx.doi.org/10.1179/136217109X415893.

[182] Khan NZ, Siddiquee AN, Khan ZA, Shihab SK. Investigations on tunneling and kissing bond defects in FSW joints for dissimilar aluminum alloys. Journal of Alloys and Compounds. 2015;648:360-367. http://dx.doi.org/10.1016/j.jallcom.2015.06.246.

[183] Panneerselvam K, Lenin K. Investigation on effect of tool forces and joint defects during FSW of polypropylene plate. Procedia Engineering. 2012;38:3927-3940. http://dx.doi.org/10.1016/j.proeng.2012.06.450.

[184] Villegas JC, Shaw LL, Dai K, Yuan W, Tian J, Liaw PK, et al. Enhanced fatigue resistance of a nickel-based hastelloy induced by a surface nanocrystallization and hardening process. Philosophical Magazine Letters. 2005;85(8):427-438. http://dx.doi.org/10.1080/09500830500311705.

[185] Gatey AM, Hosmani SS, Singh RP. Surface mechanical attrition treated AISI 304L steel: role of process parameters. Surface Engineering. 2016;32(1):69-78. http://dx.doi.org/10.1179/1743294415Y.0000000056.

[186] Seemikeri CY, Mahagaonkar SB, Brahmankar PK. The influence of surface enhancement by low plasticity burnishing on the surface integrity of steels. International Journal of Surface Science and Engineering. 2010;4(4/5/6):465-491. http://dx.doi.org/10.1504/IJSURFSE.2010.035148.

[187] Huang Y, Wan L, Lv S, Liu H, Feng J. Gradient micro-structured surface layer on aluminum alloy fabricated by in situ rolling friction stir welding. Materials & Design. 2013;52:821-827. http://dx.doi.org/10.1016/j.matdes.2013.06.026.

[188] Sánchez Egea ACAJ, Rodríguez A, Celentano D. Joining metrics enhancement when combining FSW and ball-burnishing in a 2050 aluminium alloy. Surface and Coatings Technology. 2019;367:327-335. https://doi.org/10.1016/j.surfcoat.2019.04.010.

[189] Dong P, Liu Z, Zhai X, Yan Z, Wang W, Liaw PK. Incredible improvement in fatigue resistance of friction stir welded 7075-T651 aluminum alloy via surface mechanical rolling treatment. International Journal of Fatigue. 2019;124:15-25. http://dx.doi.org/10.1016/j.ijfatigue.2019.02.023.

[190] Du C, Pan Q, Chen S, Tian S. Effect of rolling on the microstructure and mechanical properties of 6061-T6 DS-FSW plate. Materials Science and Engineering A. 2020;772:138692. http://dx.doi.org/10.1016/j.msea.2019.138692.

[191] Huang YX, Wan L, Lv SX, Zhang Z, Liu HJ. New technique of in situ rolling friction stir welding. Science and Technology of Welding and Joining. 2012;17(8):636-642. http://dx.doi.org/10.1179/1362171812Y.0000000056.

[192] Hassanifard S, Reyhani HA, Nabavi-Kivi A, Varvani-Farahani A. An experimental study of rolled friction-stir-welded aluminum 6061-T6 joints subjected to static and fatigue loading conditions. Journal of Materials Engineering and Performance. 2020;29(7):4493-4505. http://dx.doi.org/10.1007/s11665-020-04949-w.

[193] Altenkirch J, Steuwer A, Withers PJ, Williams SW, Poad M, Wen SW. Residual stress engineering in friction stir welds by roller tensioning. Science and Technology of Welding and Joining. 2009;14(2):185-192. http://dx.doi.org/10.1179/136217108X388624.

[194] Ghiasvand A, Kazemi M, Jalilian MM, Kheradmandan H. Investigation of exerted force on roller and roller width effects on residual stresses in direct and indirect rolling of FSW of SU304 steel. Journal of Stress Analysis. 2020;4(2):115-125. http://dx.doi.org/10.22084/jrstan.2020.20922.1127.

[195] Wen SW, Colegrove PA, Williams SW, Morgan SA, Wescott A, Poad M. Rolling to control residual stress and distortion in friction stir welds. Science and Technology of Welding and Joining. 2010;15(6):440-447. http://dx.doi.org/10.1179/136217110X12785889549787.

[196] Zhou L, Li GH, Liu CL, Wang J, Huang YX, Feng JC, et al. Effect of rotation speed on microstructure and mechanical properties of self-reacting friction stir welded Al-Mg-Si alloy. International Journal of Advanced Manufacturing Technology. 2017;89(9-12):3509-3516. http://dx.doi.org/10.1007/s00170-016-9318-5.